

Tectonics

RESEARCH ARTICLE

10.1002/2017TC004655

Key Points:

- We present a new tectonic scenario for the Cretaceous-Paleocene development of the mid-Norwegian Margin and the northern Vøring segment in particular
- Crustal architecture and tectonic development of the volcanic rifted mid-Norwegian Margin significantly differs from the Iberian type margins
- The development of sag basins is strongly related to inherited crustal blocks ("buffers")

Correspondence to:D. Zastrozhnov,
zastrozhe@gmail.com**Citation:**

Zastrozhnov, D., Gernigon, L., Gogin, I., Abdelmalak, M. M., Planke, S., Faleide, J. I., ... Myklebust, R. (2018). Cretaceous-Paleocene evolution and crustal structure of the northern Vøring Margin (offshore mid-Norway): Results from integrated geological and geophysical study. *Tectonics*, 37, 497–528. <https://doi.org/10.1002/2017TC004655>

Received 11 MAY 2017

Accepted 11 JAN 2018

Accepted article online 15 JAN 2018

Published online 8 FEB 2018

Cretaceous-Paleocene Evolution and Crustal Structure of the Northern Vøring Margin (Offshore Mid-Norway): Results from Integrated Geological and Geophysical Study

D. Zastrozhnov^{1,2} , L. Gernigon³, I. Gogin⁴, M. M. Abdelmalak^{1,2} , S. Planke^{1,2}, J. I. Faleide¹ , S. Eide⁵ , and R. Myklebust⁶

¹Centre for Earth Evolution and Dynamics, University of Oslo, Oslo, Norway, ²Volcanic Basin Petroleum Research (VBPR), Oslo Science Park, Oslo, Norway, ³Geological Survey of Norway (NGU), Trondheim, Norway, ⁴RPS Ichron, Northwich, UK,

⁵First Geo AS, Skøyen, Norway, ⁶TGS, Asker, Norway

Abstract We present results of a multidisciplinary study of the northern segment of the Vøring volcanic rifted margin, offshore mid-Norway. This segment represents a transitional margin domain that is less investigated compared to the adjacent segments of the margin. In order to understand the geological evolution of the study area, we performed an integrated interpretation of an extensive geological and geophysical data set. This data set includes recently acquired and reprocessed 2-D reflection seismic, published refraction data and potential field data, as well as new borehole data. Two-dimensional potential field modeling was performed to better assess the crustal architecture and evolution of the northern Vøring Margin. We then consider how crustal-scale structures and processes affected the basin formation. The outer and distal northern Vøring Margin represents a series of deep Cretaceous (Træna Basin and Någrind Syncline) and Cretaceous-Paleocene (Hel Graben) sag subbasins underlain by a significantly thinned continental crust. These subbasins developed in between structural highs (Utgard, Nyk, and Grimm Highs), which are underlain by a thicker crust and interpreted as a series of rigid continental blocks ("buffers"). In addition to the regional Late Jurassic-Early Cretaceous rifting events, we found structural evidence of local Neocomian and mid-Cretaceous extensional reactivation affecting the northern segment of the Vøring Basin. During the mid-Late Cretaceous-Paleocene, the extensional axis within the Vøring Basin province migrated sequentially northwestward to the present-day continent-ocean "boundary". We also show fundamental differences between the volcanic rifted mid-Norwegian Margin and nonvolcanic (Iberian-type) margins and how preexisting structures events can shape the evolution and architecture of the margin.

1. Introduction

The processes through which continental rifting develops into oceanic rifting is a major challenge in the Earth Sciences. The relationship between continental rifting and magmatism and the transition from rifting to spreading (e.g., the breakup stage) are still poorly understood and controversial. Important questions usually concern the following: (1) how much continental extension and thinning of the lithosphere predates the initiation of oceanic rifting (e.g., Brune et al., 2016; Huismans & Beaumont, 2011; Lavier & Manatschal, 2006; Van Avendonk et al., 2009), (2) how the rifting and breakup extension are physically and rheologically accommodated by faulting/shearing and/or igneous additions (e.g., Brune et al., 2012; Buck, 2006; Ebinger & Casey, 2001; Rosenbaum et al., 2010; Yamasaki & Gernigon, 2009), (3) the role of inheritance in rift and drift development (e.g., Harry & Bowling, 1999; Petersen & Schiffer, 2016), and (4) the fundamental magmatic and tectonic differences between "magma-poor" and volcanic rifted margins (Franke, 2013; Geoffroy et al., 2015).

In this context, we explore the crustal structure and tectonostratigraphic development of the Vøring Margin, which is a part of the mid-Norwegian Margin (Figure 1). The Vøring Margin is long recognized to be a classic example of a volcanic rifted margin. It is characterized by a long period of rifting, distal basaltic seaward dipping reflectors (SDRs), extensive distribution of mafic dikes and sills in the continental crust and sedimentary basins, and the presence of high-velocity ($V_p > 7.0$ km/s) lower crustal bodies (Abdelmalak et al., 2015, 2017; Eldholm et al., 1989; Mjelde et al., 2016; Planke et al., 1991; Skogseid et al., 2000).

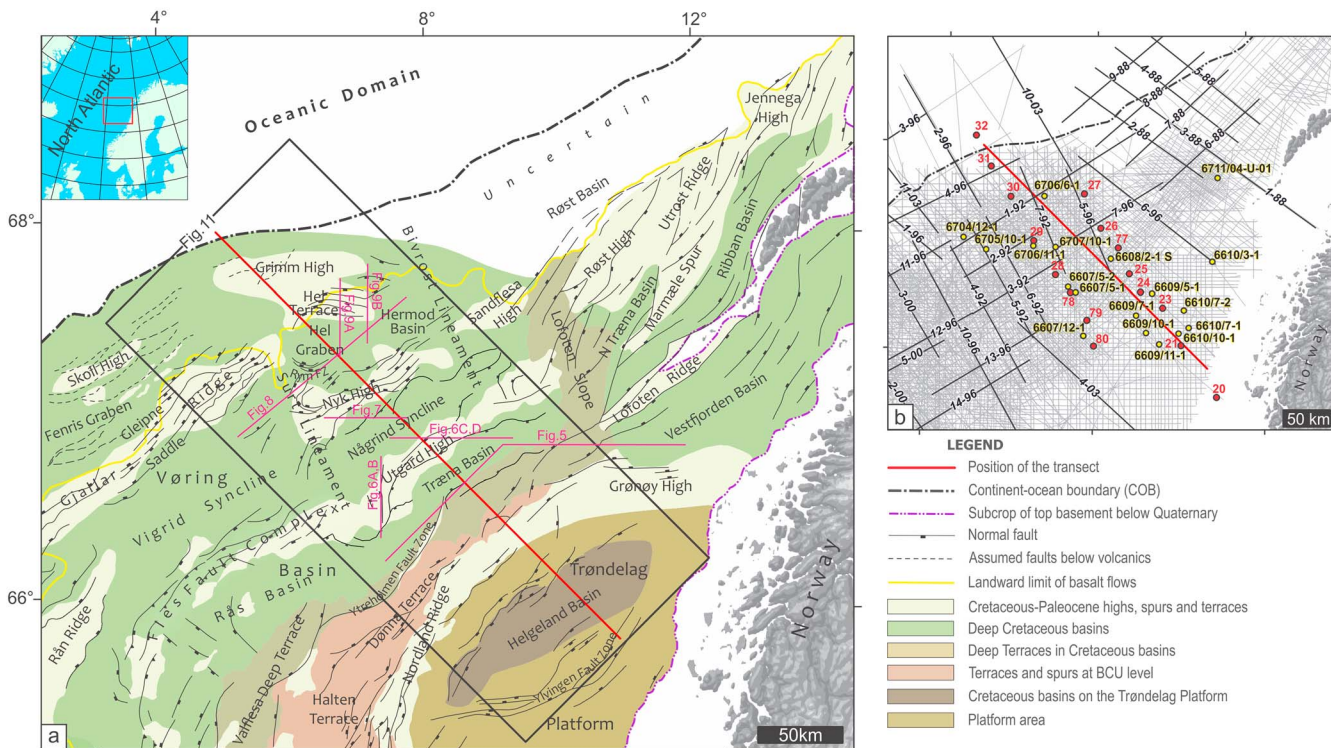


Figure 1. (a) Updated nomenclature map of the northern mid-Norwegian Margin with prebreakup structural elements. The fault pattern is mainly based on this study and modified from Blystad et al. (1995) and Gernigon et al. (2003). Locations of seismic close-ups are shown in purple solid lines. Extent of isochore maps is defined by black rectangle. (b) Geological and geophysical data set used in this study: Red circles = expended spread profiles (centers), solid black lines = ocean bottom seismometers profiles, solid light gray lines = reflection seismic, and yellow circles = main wells used in this study.

The northern part of the Voring Margin represents a specific transitional structural domain bounded by two prominent transfer zones—the Surt and Bivrost Lineaments (Figure 1a). However, this particular segment of the Voring Margin was poorly documented and less studied in terms of prebreakup tectonic evolution and crustal architecture. The main period of data acquisition and interpretation that resulted in the development of the tectonostratigraphic framework of this segment occurred two decades ago. This geophysical and geological material has been reviewed and summarized in the context of regional tectonics (Blystad et al., 1995; Brekke, 2000; Lundin et al., 2013; Mjelde et al., 1998; Mosar, 2000; Mosar et al., 2002; Osmundsen et al., 2002; Planke et al., 1991; Skogseid et al., 1992; Tsikalas et al., 2008). Only a few semi-regional case studies focus on and document the Late Cretaceous-Paleocene rifting event preceding the breakup (Fjellanger et al., 2005; Gernigon et al., 2003; Imber et al., 2005; Mogensen et al., 2000; Ren et al., 2003, 1998). Other studies have used published data sets and materials to underpin potential field modeling exercises (Ebbing et al., 2006; Kusznir et al., 2005; Maystrenko et al., 2017; Scheck-Wenderoth et al., 2007; Theissen-Krah & Rupke, 2010; Walker et al., 1997; Wangen et al., 2011).

Various controversial scenarios have been proposed to explain the dynamic and depositional evolution of the Voring Margin and its associated basins. The most recent studies have suggested some similarities with the Iberian (magma-poor) type of passive margins (Lundin & Doré, 2011; Péron-Pinvidic & Osmundsen, 2016; Reynisson et al., 2010; Rüpke et al., 2013) implying the presence of relatively wide, serpentized/exhumed mantle domains in the central, distal, and volcanic parts of the margin. In contrast, other publications consider fundamental differences with magma-poor margin (Iberian type) highlighting the role of crustal inheritance and rift duration on passive margin development and showing that there are no clear prerequisites and clear evidence to support a broad zone of mantle exhumation/serpentization within the mid-Norwegian Margin (Abdelmalak et al., 2017; Gernigon et al., 2003, 2004, 2015; Maystrenko et al., 2017; Nirrengarten et al., 2014; Petersen & Schiffer, 2016; Theissen-Krah et al., 2017). One of the debate concerns the origin and geological interpretation of the strong crustal reflections underlying mostly Cretaceous highs and basins in the distal and outer domains of the margin. This is a key aspect to consider in defining a model of the development of

the mid-Norwegian Margin and the Vøring segment in particular. A better combination of multidisciplinary geological data sets (refraction and reflection seismic, gravity and magnetic, biostratigraphy/lithostratigraphy, structural geology, tectonic and potential field modeling, etc.) is therefore necessary to validate both sedimentary and crustal interpretations (see Saltus & Blakely, 2011, for a discussion).

In this contribution, we use new and reprocessed seismic data sets, combined with recently released and revised well biostratigraphy, in order to refine the basin architecture and the Cretaceous-Paleocene tectonic evolution of the northern Vøring Margin. Over the last decade, a new generation of long-offset, high-quality seismic reflection profiles covering the entire mid-Norwegian Margin has permitted an improvement in the imaging of the deep basin structures and allowed better regional seismic interpretation. Our seismic reflection interpretation is compared with available ocean bottom seismometers (OBS) data and expanded spread profiles (ESPs) and combined with a potential field modeling along a representative NW-SE oriented crustal transect across the northern Vøring Margin. This multidisciplinary approach allows us to evaluate the properties of the deep structures beneath the sedimentary cover and test hypotheses about the style of crustal deformation and sedimentation in a poly rifted volcanic margin setting. We finally propose and discuss a crustal and tectonic scenario for the rifted margin evolution.

2. Regional Setting

The present structure of the Vøring Margin off mid-Norway is a result of several post-Caledonian extensional episodes culminating with the complete separation between Norway and Greenland in the earliest Eocene (Brekke, 2000; Faleide et al., 2008; Talwani & Eldholm, 1977). The Vøring Margin can be divided into a series of second-order structures (basins, highs, grabens, etc.) (Figure 1a) formed during Late Jurassic-Early Cretaceous and Late Cretaceous-Paleocene rifting (Blystad et al., 1995). Additional extensional events took place in mid-Cretaceous time (Bjørnseth et al., 1997; Gernigon et al., 2003; Lundin & Doré, 1997; Pascoe et al., 1999; Roberts et al., 2009) but is still a matter of debate because some authors believe that the mid-Cretaceous period was dominantly a quiet tectonic period (Færseth, 2012; Færseth & Lien, 2002). The Late Cretaceous-Paleocene rifting phase, which culminated in continental breakup near the Paleocene-Eocene transition (56 Ma), was associated with extensive and voluminous magmatic activity (Eldholm et al., 2002). This large magmatic event is traditionally correlated with the arrival of the Icelandic mantle “plume” (Skogseid et al., 2000) and/or independent sublithospheric processes (Foulger, 2010; Meyer et al., 2007; Simon et al., 2009; van Wijk et al., 2001).

The postbreakup evolution of the Vøring Margin is characterized mainly by thermal cooling and regional subsidence of the sedimentary basins (Brekke, 2000; Faleide et al., 2008). A mid-Cenozoic compressional event is also expressed by a number of inversion structures (domes/arches, reverse faults, etc.), which are likely the result of a compressive stress dominantly induced by ridge push (Doré et al., 2008; Vågnes et al., 1998). The final development of the margin is closely linked with Northern Hemisphere glaciation events, when large Plio-Pleistocene depocenters expanded over the area, increasing the regional subsidence and tilt of the margin (Faleide et al., 2008; Hjelstuen et al., 1999; Rise et al., 2005).

The northern Vøring Margin segment, which forms the focus of this study, is located west of the Nordland region onshore Norway (Figure 1). The Trøndelag Platform, which defines the proximal part of the margin segment, is a large and shallow platform containing post-Caledonian Late Paleozoic to Late Mesozoic basins (Figures 1 and 4a). The distal and outer parts of the Vøring Basin province are characterized by NE-SW oriented structural basin highs (e.g., the Utgard High and the Nyk High) and deep subbasins (e.g., the Traena Basin, the Någrind Syncline, and the Hel Graben) (Figures 1 and 4a). The northern Vøring Basin is bounded by the Surt and Bivrost Lineaments defined between the adjacent central Vøring Margin segment and the Lofoten Margin to the north (Figure 1). The transition to the outer margin domain is strongly affected by Late Cretaceous-Paleocene extensional deformation within the so-called Grimm-Rym-Nyk structural “ring” which resulted in the formation of the deep Paleocene Hel Graben and the newly defined Hermod Basin (Figure 1). The outer domain is outlined by the Paleocene Hel Terrace and Grimm High; the latter is covered by relatively thin breakup-related volcanic sequences and is interpreted as a deep-seated structural high (Abdelmalak, Planke, et al., 2016).

3. Data Set and Methods

We interpreted a large set of high-quality seismic reflection lines acquired and processed by TGS (Figure 1b). The seismic data are time migrated with a positive amplitude at the seabed and are of good to excellent

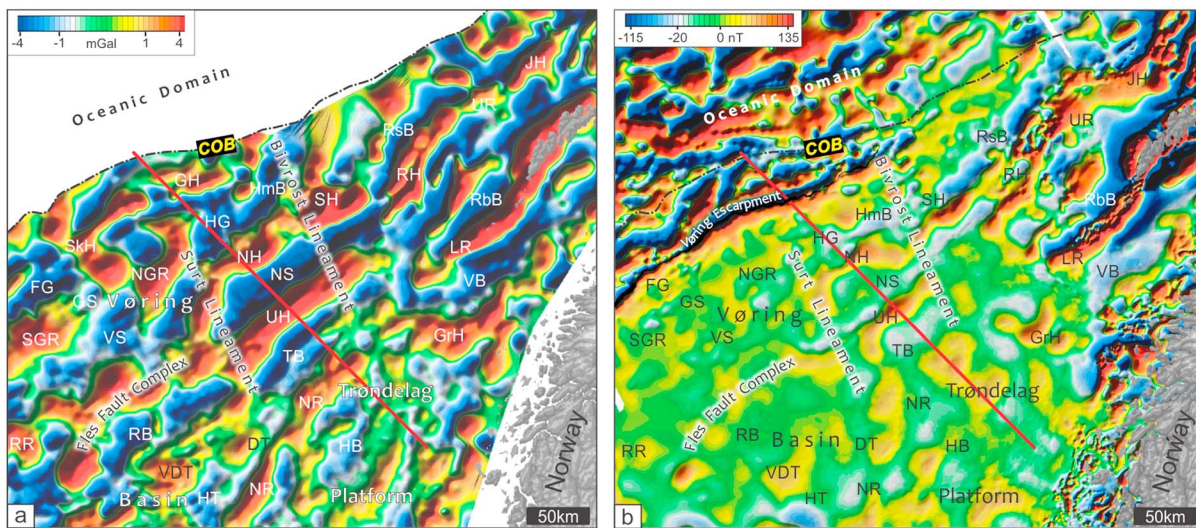


Figure 2. Potential field data for the northern Vøring Margin. (a) The 50 km high-pass-filtered Bouguer data. (b) The 50 km high-pass-filtered magnetic data. COB = continent-ocean “boundary”, DT = Donna Terrace, FG = Fenris Graben, GH = Grimm High, GS = Gleipne Saddle, GrH = Grønøy High, HB = Helgeland Basin, HG = Hel Graben, HT = Halten Terrace, HmB = Hermod Basin, LR = Lofoten Ridge, NGR = North Gjallar Ridge, NH = Nyk High, NS = Någrind Syncline, JH = Jennega High, RB = Rås Basin, RH = Røst High, RR = Rån Ridge, RbB = Ribban Basin, RSB = Røst Basin, SGR = South Gjallar Ridge, SH = Sandflesa High, SkH = Skoll High, TB = Træna Basin, UH = Utgard High, UR = Utrøst Ridge, VB = Vestfjorden Basin, VDT = Valflesa Deep Terrace, VS = Vigrid Syncline. Data courtesy of TGS.

quality, although some deterioration occurs below sill intrusions. The potential field data were provided and processed by TGS. Well formation tops were obtained from the Norwegian Petroleum Directorate (NPD) (NPD factpages, 2017) and the Norwegian Offshore Stratigraphic Lexicon (NORLEX) group (Gradstein et al., 2010). The raw results of biostratigraphic analyses and wireline logs for well 6608/2-1S have been provided by the NPD but have been reevaluated by RPS Ichron (see Appendix A and Figure A1).

The seismic data set has been jointly interpreted together with potential field data (Figure 2) and published crustal-scale velocity data (Figure 1b) derived from ocean bottom seismometers (OBS) and expanded spread profiles (EPS) surveys (Digranes et al., 1998; Mjelde et al., 1998; Planke et al., 1991).

3.1. Seismic Interpretation

The regional seismic interpretation has been carried out using IHS Kingdom software. The line spacing of the final data set (Figure 1b) ranges from 0.2 to 2 km, which was sufficient enough to confidently tie the different seismic units mapped in this study. We interpreted a set of regional Cretaceous-early Cenozoic seismic horizons over the entire northern Vøring Margin (Figure 3). These units were correlated with the well database. The final regional horizons include the following: the Base Cretaceous Unconformity (BCU), mid-Albian (?) (MA), mid-Cenomanian (MC), Top Turonian (TT), intra mid-Campanian (IMC), the Base Tertiary Unconformity (BT), and Top Paleocene (TP) (Figure 3). Additionally, several pre-Cretaceous reflections were picked on the Trondelag Platform, while Top Santonian (TS) and Base Late Pliocene (BLP) have been interpreted locally. We constructed a number of time-thickness (isochore) maps (Figure 11) in order to highlight the regional configuration of the main depocenters, their migration through time and space, and their relationship with the deep crustal architecture of the margin.

The crustal structure for the proximal part (Trondelag Platform) was obtained from the reflection data where the interpreted top crystalline basement (TB) marker can be reliably identified over the area and tied with wells. To further constrain the crustal structure of the deep Vøring Basin, we compared the seismic interpretation with the top basement grid from a 3-D lithospheric model (previously published by Scheck-Wenderoth and Maystrenko, 2011). In the areas where the top basement grid crosses confidently interpreted sedimentary successions, we moved it down to a depth level consistent with the seismic observation since the new and reprocessed long-offset seismic data allow us now to more confidently identify deeper strong midcrustal reflections in the sedimentary basin. Most likely deeper than 10–11 s two-way travel time (TWT), the Moho is barely recognized on the seismic reflection data; as a result, we used OBS and ESP data and potential field modeling results to identify and map the Moho.

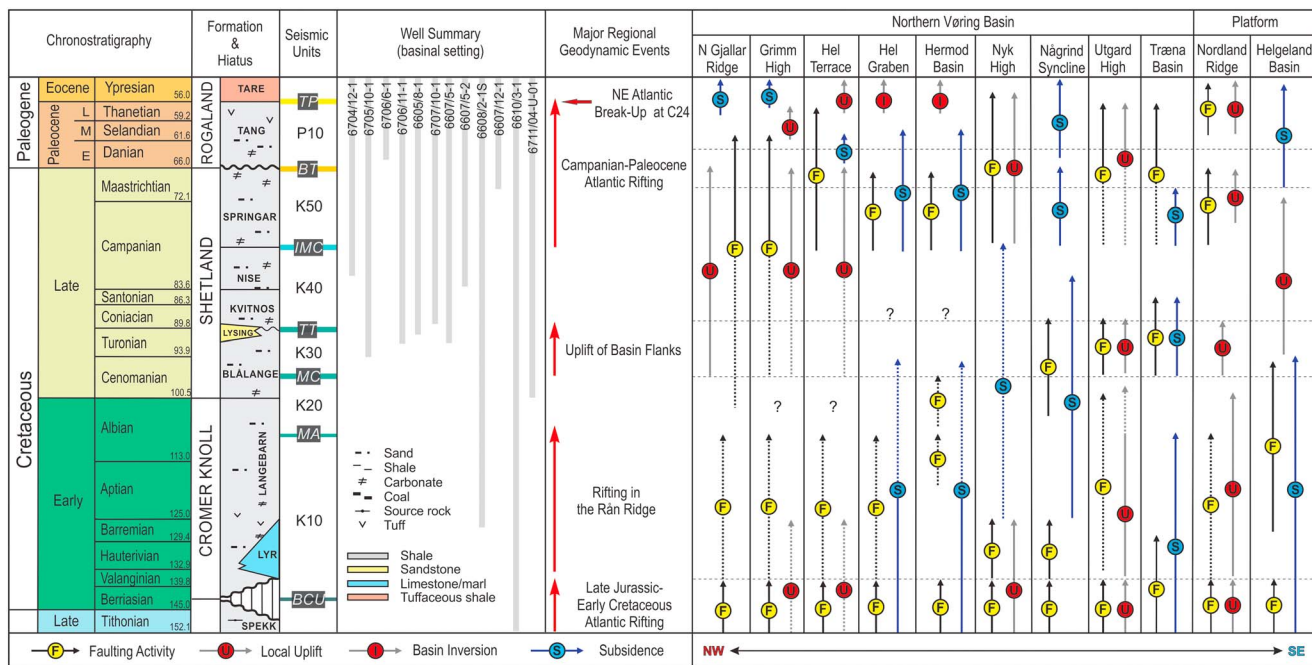


Figure 3. Tectonostratigraphic summary of the study area. Time scale after Cohen et al. (2013).

3.2. Potential Field Data

The 50 km high-pass-filtered Bouguer gravity anomaly map processed by TGS (Figure 2a) reveals a complex pattern of high- and low-amplitude anomalies along the margin. High-pass filtering of the data makes it possible to dissociate gravity anomalies caused by shallow basement structures from density variations in the deepest crust and/or the upper mantle. Cutoff wavelengths of 50 km emphasize density contrasts with source depth usually deeper than 10 km.

The 50 km high-pass-filtered magnetic data (Figure 2b) are based on the Mid-Norway Aeromagnetic Compilation by TGS, including the most recent ship track and aeromagnetic surveys in the Vøring Margin. Within the continental domain, these data allowed identification of the main deep-sourced magnetic anomalies. It provides information about the deep continental basement rocks expected below the nonmagnetic sedimentary cover. The 50 km high-pass-filtered potential field data were included in the seismic project, scaled to two-way travel time, converted to pseudohorizons, and displayed on the seismic lines to facilitate the joint interpretation of the seismic, gravity, and magnetic data.

3.3. Potential Field Modeling of the Northern Vøring Transect

Potential field modeling is a useful technique to evaluate and check further basement depth, nature, and properties. To illustrate the crustal configuration of the northern Vøring Margin, a 2-D potential field modeling has been carried out along a characteristic NW-SE section striking from the Helgeland Basin on the Trøndelag Platform up to the continent-ocean “boundary” (Figure 4). This section illustrates the main crustal configuration interpreted beneath the main structural highs and subbasins described in this study. The forward modeling has been carried out using the commercial software GM-SYS integrated within the GEOSOFT Oasis Montaj software. The modeling itself is based on the conventional and original method of Talwani (1973), where sets of irregular polygons with different physical properties along a 2-D transect create magnetic and gravity signals that are then compared with the observed potential field values. The geometry and properties of the polygons are changed accordingly until the best fit between the observed and calculated signal is achieved.

The 2-D margin transect was first depth converted using hiQbe™ Mid-Norway, a regional high-quality seismic velocity cube covering the entire mid-Norwegian Margin (<http://www.first-geo.com/products/hiqbe/norway>). The velocity cube has been compiled from 536 seismic stacking velocity data sets, including the stacking velocities along the transect, employing proprietary and industry standard geostatistical methods. The

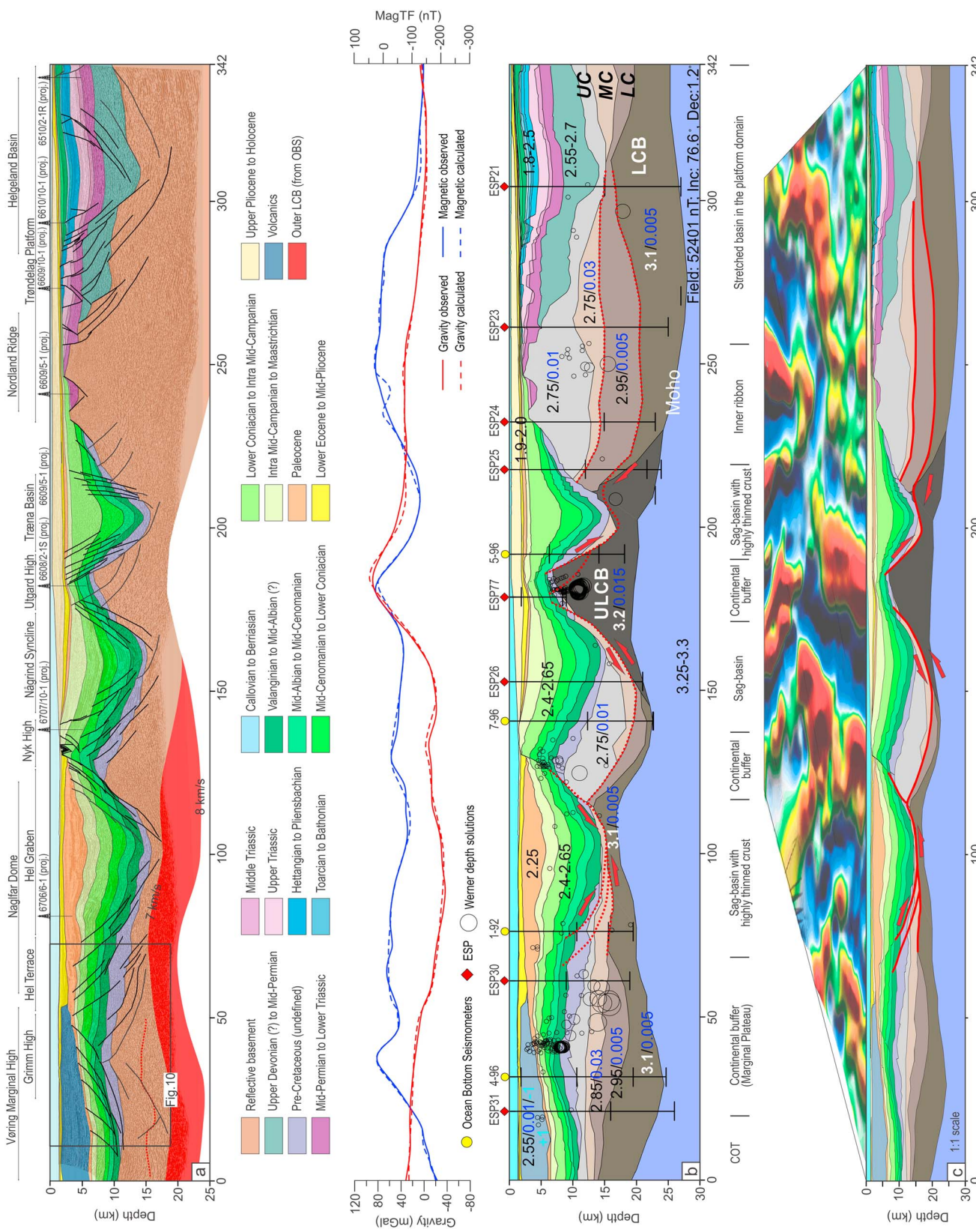


Figure 4. Crustal transect across the northern Voring Margin derived from (a) seismic observations and (b) potential field modeling (see Figure 1a for location). (c) Similar section at 1:1 scale with structural features discussed in the text. In the northern Voring Margin we propose a model of crustal boudinage, where sag basins with thin and very thin crust are separated by rigid continental buffers. LC = lower crust, LCB = lower crustal body, UC = upper crust, MC = middle crust. Note the differences between the interpreted and modeled transect in the central Hel Graben, where we have to remove pre-Cretaceous sediments in order to get better fit with the gravity.

stacking velocities are calibrated to 230 check shots from wells, compensating for delta anisotropy—a parameter describing the near-vertical P wave propagation (Thomsen, 1986). At depths below well control, the delta anisotropy cannot be calculated directly from the well check shot. Calibration was then achieved by extrapolating the delta anisotropy downward in such a way that the hiQbe™ velocities are comparable to those derived from seismic refraction modeling of OBS data (e.g., Ni Dheasúna et al., 2012).

The software TecMod 2-D was also used to estimate total and tectonic subsidence rates for a series of rifting episodes in the Træna Basin calculated with forward modeling and classic backstripping approach. Kinematic, isostatic, and thermal principles of these approaches and their comparison are described in detail by Rüpke et al. (2008, 2010), Theissen-Krah and Rüpke (2010), and Clark et al. (2014).

4. Results

4.1. Geological Structure, Seismic Interpretation, and Correlation With Potential Field Data Along the Transect

Transect in Figure 4a illustrates the main basin and structural configuration of the northern Vøring Margin. The 342 km long transect strikes NW-SE from the Ylvingen Fault Zone at the Helgeland Basin on the Trøndelag Platform across the Vøring Basin and terminates close to the expected continent-ocean “boundary”.

The Trøndelag Platform defines the proximal and shallower part of the margin segment and shows Devonian-Early Carboniferous? to Jurassic basins (Blystad et al., 1995; Osmundsen et al., 2002) bounded to the east by the Caledonian basement that crops out in the onshore part. The structure of the thick Late Paleozoic basin (up to 6 km) is dominantly controlled by fault systems (Figure 4), which were possibly initiated during post-Caledonian orogenic collapse and then sequentially reactivated during Carboniferous?-Permian rifting episodes (e.g., Doré et al., 1999). To the west, this Late Paleozoic basin extends to a prominent basement horst lying at the northern prolongation of the Nordland Ridge (Figures 1a and 4a). Due to high density, this basement horst coincides with a pronounced gravity anomaly observed at that level (Figures 2b and 4b). We were able to tie a top basement marker to well 6609/7-1, where this horst structure was drilled and basement rocks were reached at a shallow level of 1,912 m (NPD factpages, 2017). The recovered rocks predominantly consist of pre-Cambrian quartzite and other low-medium-grade metamorphic rocks with evident sedimentary origin (Slagstad et al., 2011).

Later Mesozoic faulting activity in the area generated second-order half-grabens, grabens, and horst structures. Triassic to Jurassic sediments covered the deep Late Paleozoic basin and the basement horst and were subsequently peneplained in the Nordland Ridge at the BCU level. The superimposed Helgeland Basin (Figure 4a) observed in the inner platform contains a mainly Early Cretaceous sedimentary fill (Blystad et al., 1995; Brekke, 2000).

Our seismic interpretation shows basinward dipping fault systems at the northwestern flank of the Nordland Ridge/Grønøy High (Figure 5). Those faults controlled the Cretaceous evolution of the narrow and deep Træna Basin, which was poorly imaged by the previous seismic data sets. Compared to surroundings, the Træna Basin is characterized by NE trending negative gravity and magnetic anomalies (Figure 2). Despite a uniformly deep configuration of the basin along its strike, we observed a subtle increase of the magnetic and gravity signal (Figure 2) toward the Lofoten-Vesterålen Margin, which coincides with a strong seismic reflection underlying the deep-seated pre-Cretaceous fault blocks (Figure 5). The transition to the adjacent deep Rås Basin is marked by prominent north trending, relatively strong, positive gravity and magnetic anomalies (Figures 2 and 5) lying in the prolongation of the Surt Lineament, which is interpreted as an old inherited basement structure (Blystad et al., 1995). Our interpretation highlights a deep basin configuration (BCU at 7–8 s in the axial part; Figure 5). Regional mapping and our revised calibration suggest thin Lower Cretaceous successions (about 1 s TWT) underlying thick Coniacian to mid-Campanian sequences (Figure 5).

The northwestern flank of the Træna Basin is defined by the Utgard High. This prominent basement high, which is characterized by a strong NE trending gravity anomaly, can be divided into two segments (Figure 2a). The gravity anomaly is clearly connected to a prominent high-amplitude reflection observed in the deep part of the high (Figure 6). We have to note here that the observed reflection represents some local deep features and we were not able to establish any direct and spatial connection with the notable and similar deep T -Reflection defined and described farther west in the outer part of the Vøring Basin (see Abdelmalak

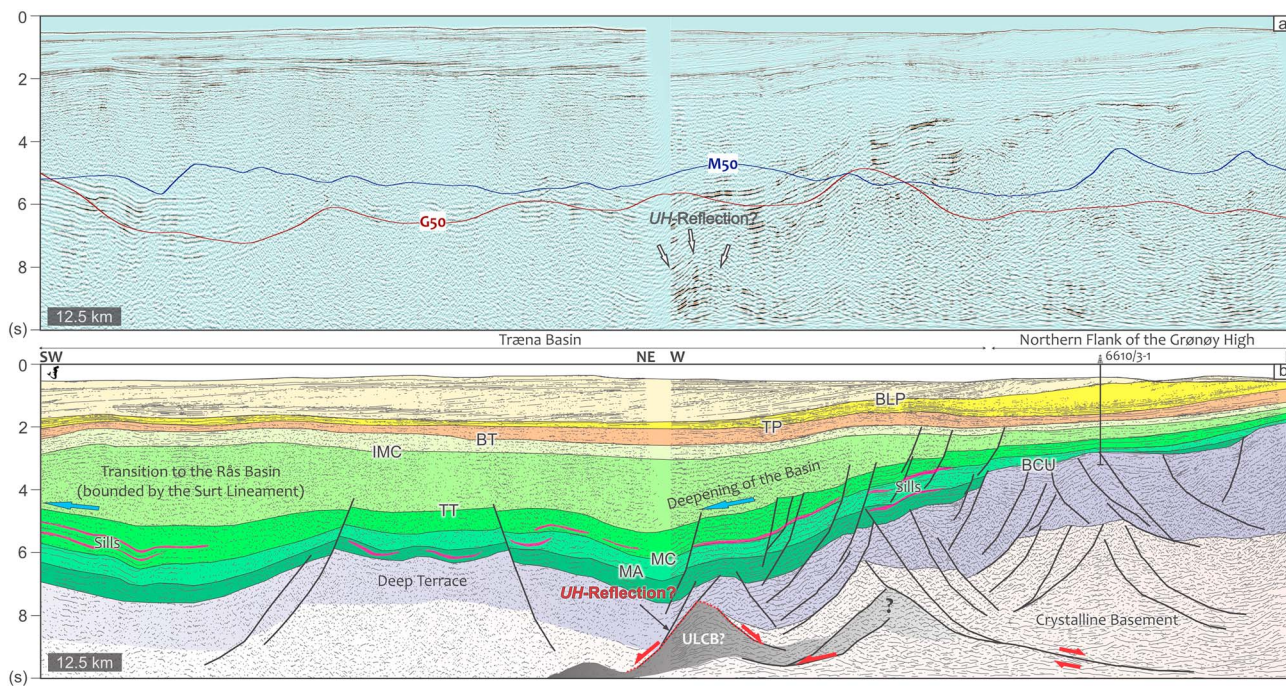


Figure 5. Composite seismic line showing configuration of the deep Træna Basin with relatively thin Lower Cretaceous and thick Upper Cretaceous successions: (a) uninterpreted and (b) interpreted. Pre-Cretaceous fault blocks are underlain by the deep crustal reflection associated with the increase of a gravity signal and could be related to a basin continuation of the ultrahigh-density lower crustal body (ULCB) observed in the Utgard High (see Figures 4b and 6). G50 = 50 km high-pass-filtered Bouguer anomaly pseudohorizon; M50 = 50 km high-pass-filtered magnetic data pseudohorizons. The common legend for the sedimentary part is shown in Figure 4. The abbreviations for the horizons are given in section 3.1. The location of the seismic line is shown in Figure 1a. Data courtesy of TGS.

et al., 2017; Gernigon et al., 2003). In this study, we named it the *UH* (Utgard High)-Reflection to specify the difference from the *T*-Reflection. In the southern segment of the Utgard High, the *UH*-Reflection shows a gently undulating configuration at a relatively deep level (7.5–8 s TWT) (Figures 6a and 6b). In the northern segment the *UH*-Reflection shallows up to 5 s TWT, where it fits well with a stronger gravity signal (Figures 6c and 6d). In its shallow part, the *UH*-Reflection is disrupted and displaced both by a series of Late Jurassic-Early Cretaceous (and older?) and Late Cretaceous-Paleocene landward dipping normal fault systems (Figures 6b and 6d) that control the structural development of the Utgard High (Blystad et al., 1995; Skogseid et al., 1992).

The recent drilling results (well 6608/2-1S) in the northern Utgard High indicated that the BCU is much deeper than was previously thought (Blystad et al., 1995; Brekke, 2000), with sediments from the Lower Cretaceous Lyr Formation still preserved at the well bottom (5.6 km; see Appendix A). Accordingly, we could not expect much pre-Cretaceous sediments in the northern Utgard High (1–1.5 km thick) if we assume the potential basement origin of the *UH*-Reflection (see also modeling results and discussion). Furthermore, our biostratigraphic reinterpretation of well 6608/2-1S (see Appendix A and Figure A1) suggests a significant thickness of the Lower Cretaceous sediments (>1.1 km) and a thinner Turonian interval in comparison to the previous predrilling interpretations (Blystad et al., 1995; Brekke, 2000). The Turonian interval of the well is considered to be either condensed or representative of a stratigraphic unconformity. Our biostratigraphic analysis of well 6608/2-1S confirms the presence of Middle-Late Turonian biomarkers and also suggests a lack of Early Turonian assemblages. Tentatively, we explain the lack of early Turonian biomarkers by the presence of an unconformity within the early and partly middle Turonian intervals apparently missing from the section.

Farther to the northwest, the Utgard High flanks the Någrind Syncline, a 10 km thick deep Cretaceous sag basin better imaged now with the new seismic data (Figure 7). The Surt Lineament separates the Någrind Syncline from the Vigrid Syncline in the southwest, whereas its northern continuation is limited by the Bivrost Lineament (Figure 1a). Like the Træna Basin, the Någrind Syncline also corresponds to strong negative gravity and magnetic anomalies (Figure 2). The tectonic history of the Någrind Syncline is strongly related to the Late Jurassic to Paleocene development of the adjacent highs (the Nyk and Utgard Highs) and the

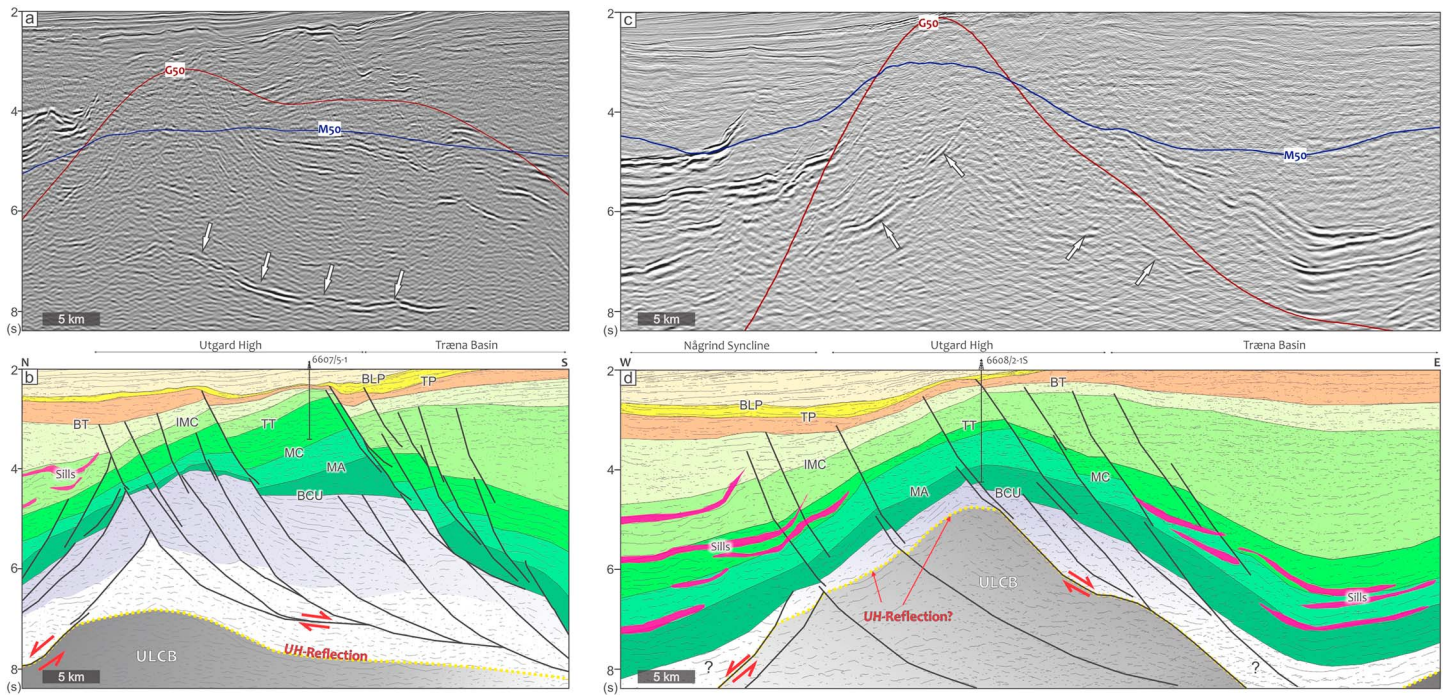


Figure 6. Structure of the Utgard High and configuration of the ULCB. Southern segment: (a) uninterpreted and (b) interpreted seismic sections. Northern segment: (c) uninterpreted and (d) interpreted seismic sections. White arrows on the uninterpreted sections point at the *UH-Reflection* interpreted as the top of the ULCB. Note the significant increase of the gravity and magnetic signals (G50 and M50, respectively) in the northern segment of the high. The common legend for the sedimentary part is shown in Figure 4. The abbreviations for the horizons are given in section 3.1. The location of the seismic line is shown in Figure 1a. Data courtesy of TGS.

structural evolution of the flanking/bounding transfer zones (e.g., the Surt and Bivrost Lineaments) (Blystad et al., 1995; Brekke, 2000). We found evidence that the Jurassic-early Cretaceous rifting did not terminate here at BCU level (Berriasian, according to Dalland et al., 1988) but prolonged into the Neocomian (Barremian-Aptian?) time. The early and late synrift wedges of Jurassic-Early Cretaceous and possible Neocomian age respectively were controlled by normal faulting on the flank of a deep horst lying below the Nyk High (Figures 4a and 7).

The nearly NE trending positive gravity and magnetic trend in the Nyk High correlates well with a shallow basement high observed at that level (Figure 2). The anomalies curve in an almost southern direction within the Surt Lineament mimicking the deep structural configuration. The dominant and shallower structural style of the Nyk High at the present day represents the uplifted and eroded footwall of a rifting system, which initiated in Late Cretaceous time and was active during most of the Paleocene (Gernigon et al., 2003; Mogensen et al., 2000; Ren et al., 2003). Rift shoulder uplift of the Nyk High was concomitant with a significant subsidence of the adjacent Någrind Syncline, which is not particularly affected by classic rotated fault blocks. The ongoing extension during the Paleocene promoted severe collapse of the western flank of the Nyk High, thus creating significant accommodation space resulting in preservation of a thick Paleocene succession observed and drilled (e.g., well 6706/6-1) in the Hel Graben (Figure 4a). Later Paleocene-early Eocene minor sinistral transpressional reactivation complicated the fault pattern within the Nyk High (Imber et al., 2005).

There is still an ongoing debate on the Late Cretaceous-Paleocene development of the Hel Graben. The more recent interpretations rely on the controversial stratigraphic analysis of well 6706/6-1. The NPD claims that there is at least 1,400 m of Paleocene deposits in the well (NPD factpages, 2017) with no penetration within Upper Cretaceous sediments expected at that level in predrilling interpretation (Blystad et al., 1995; Ren et al., 2003). In contrast, the NORLEX team (Gradstein et al., 2010, and well report at <http://www.nhm.uio.no/norlex>) interprets the same section as comprising Upper Cretaceous Shetland Group sediments, suggesting only 200 m of Paleocene sediments in the well; this interpretation implies that the Hel Graben is dominantly a Late Cretaceous rather than Paleocene synrift feature (e.g., Fjellanger et al., 2005). Our own seismic tie

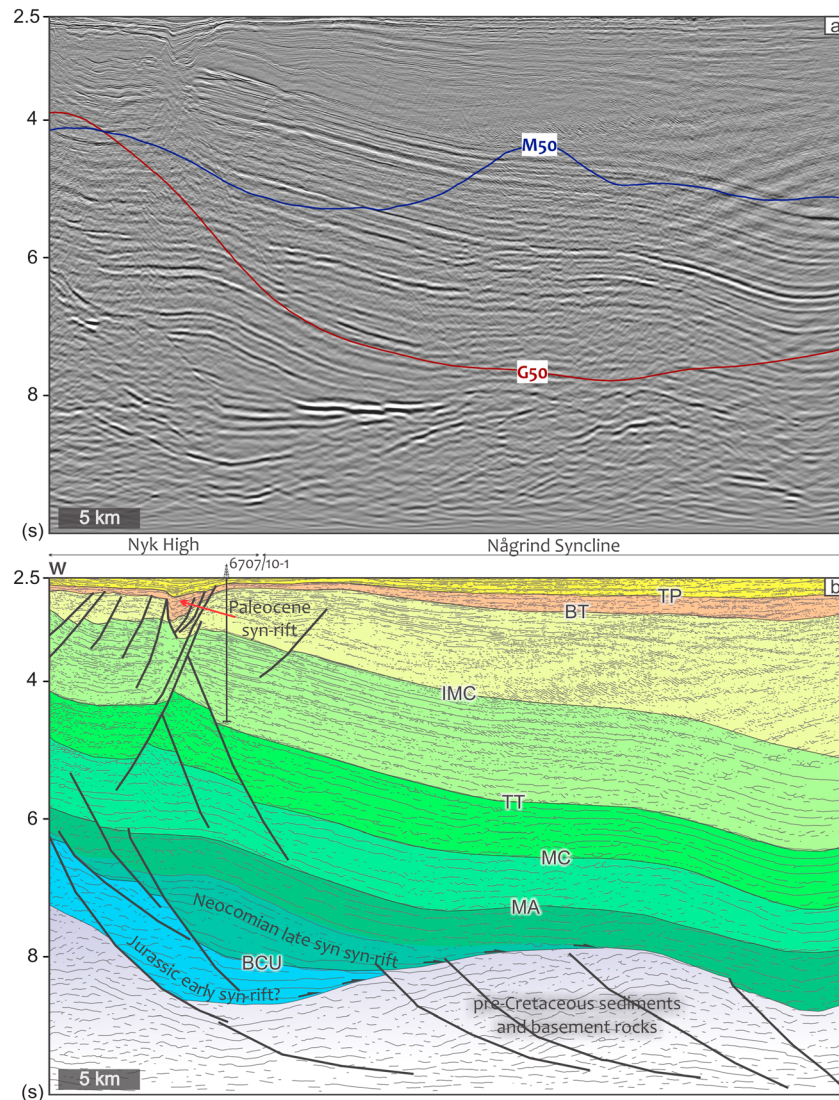


Figure 7. Seismic line across the Någrind-Nyk segment of the study area: (a) uninterpreted and (b) interpreted. Here we can recognize Jurassic and Neocomian synrift wedges developed on the eastern flank of the Nyk High. The deep and old synrift sequences are controlled by an east dipping faults. Maastrichtian-Paleocene rifting in the area was associated with west dipping faulting, the uplift of the Nyk High, and significant subsidence of the Någrind Syncline, where a large depocenter was formed. The common legend for the sedimentary part is shown in Figure 4. The abbreviations for the horizons are given in section 3.1. The location of the seismic line is shown in Figure 1a. Data courtesy of TGS.

from the adjacent Vigrid Syncline into the Hel Graben across the Rym Fault Zone (Figure 8) does support the presence of thick Paleocene sediments in the Hel Graben. However, our interpretation of the deepest parts of the structure is less confident due to poor imaging caused by extensive distribution of magmatic intrusives, making our assessment of the pre-Paleocene structure more speculative. However, seismic imaging locally allows to estimate the relative depth of the BCU (Figure 8).

The Hel Graben is characterized by a rounded negative gravity anomaly (Figure 2a). It laterally passes into the Paleocene Hermod Basin interpreted as a separate subbasin in this study (Figures 1a and 8). The limit between the two subbasins is characterized by a deep-seated high (Figure 8). The gravity pattern shows that the Hermod Basin may extend northeast toward the outer Lofoten Margin (Figure 2a) and possibly merge with the Røst Basin as recently suggested by Maystrenko et al. (2017). The 3-D potential field modeling of Maystrenko et al. (2017) suggests that thick Late Cretaceous-Paleocene sequences (undifferentiated) may likely exist underneath the Lofoten lava inner flows.

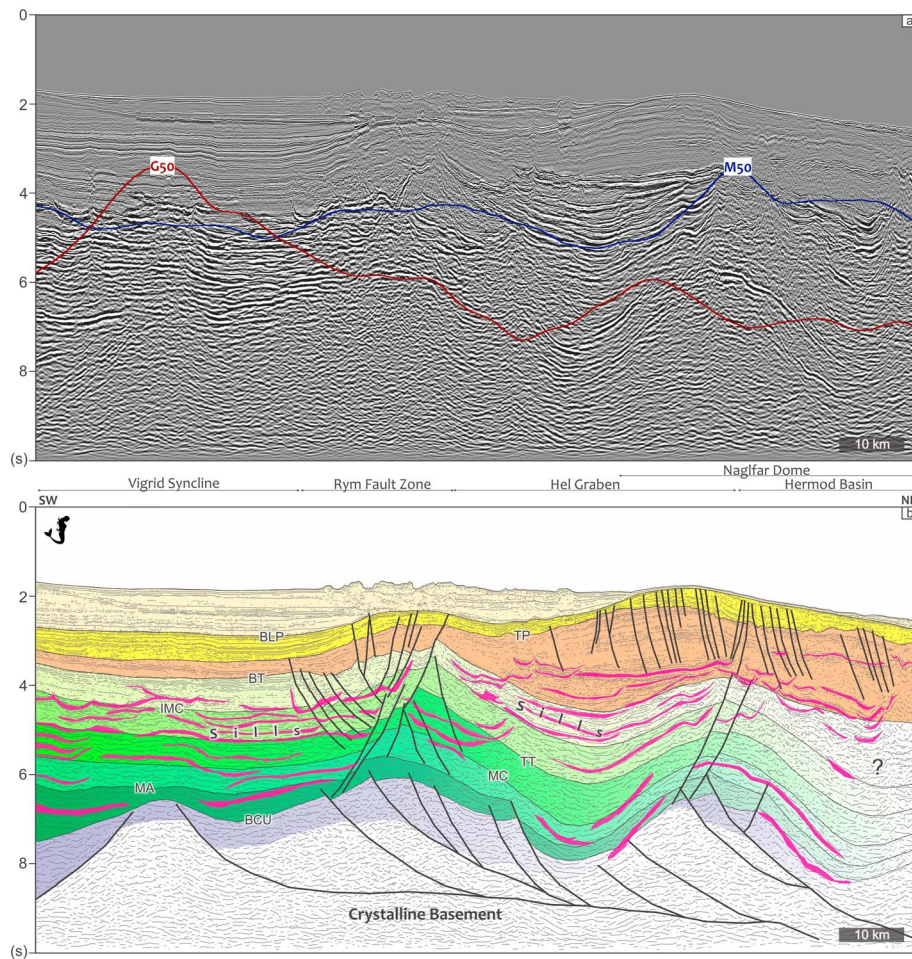


Figure 8. Seismic tie from the Vigrid Syncline to the Hel Graben revealing the deep configuration of the basin formed underneath thick Paleocene successions: (a) uninterpreted and (b) interpreted lines. The Hel Graben and the adjacent Hermod Basin are structurally divided by a deep-seated structural high. The common legend for the sedimentary part is shown in Figure 4. The abbreviations for the horizons are given in section 3.1. The location of the seismic line is shown in Figure 1a. The 50 km high-pass-filtered Bouguer gravity (G50) and magnetic (M50) anomalies are shown. Data courtesy of TGS.

The northern boundary of the Hel Graben is defined by the Hel Terrace. Together with the Hermod Basin, this is also a newly defined structural element. It is characterized by a series of southward dipping Late Cretaceous-Paleocene growth faults (Figure 9a) possibly decoupled and developing over overpressured mobile shales widely distributed in Lower to mid-Cretaceous intervals in the deep Vøring Basin (Brekke et al., 1999; Dalland et al., 1988; Vergara et al., 2001). Farther northeast, the northern flank of the Hel Terrace is characterized by a graben-like feature with clear synrift Paleocene seismic wedges postdating the main Late Cretaceous-Paleocene extensional phase leading to the formation of the Hel Graben (Figure 9b). The new seismic data also suggest that the footwall of the Hel Terrace was exposed and peneplained during this period. Notably, we discovered evidence of earlier pulses of magmatism (intra-Paleocene) in the Hermod Basin compared to the main early Eocene volcanic event recognized in the Vøring Marginal High. This early phase of magmatism is witnessed by older vent complexes that developed in the Paleocene successions and genetically linked with deeper sill intrusions (Figure 9b).

The subbasalt Grimm High (Figures 4 and 10) has been defined based on a previous integrated seismic-gravity-magnetic interpretation of the volcanic margin (Abdelmalak, Planke, et al., 2016). It coincides with a gravity high that correlates with a positive magnetic anomaly, suggesting a shallow basement beneath the basalt (Figures 2 and 10). The anomalies also correlate well with a structural high interpreted at the top and base basalt levels at the Vøring Marginal High (Abdelmalak, Planke, et al., 2016). The Grimm High has a thin

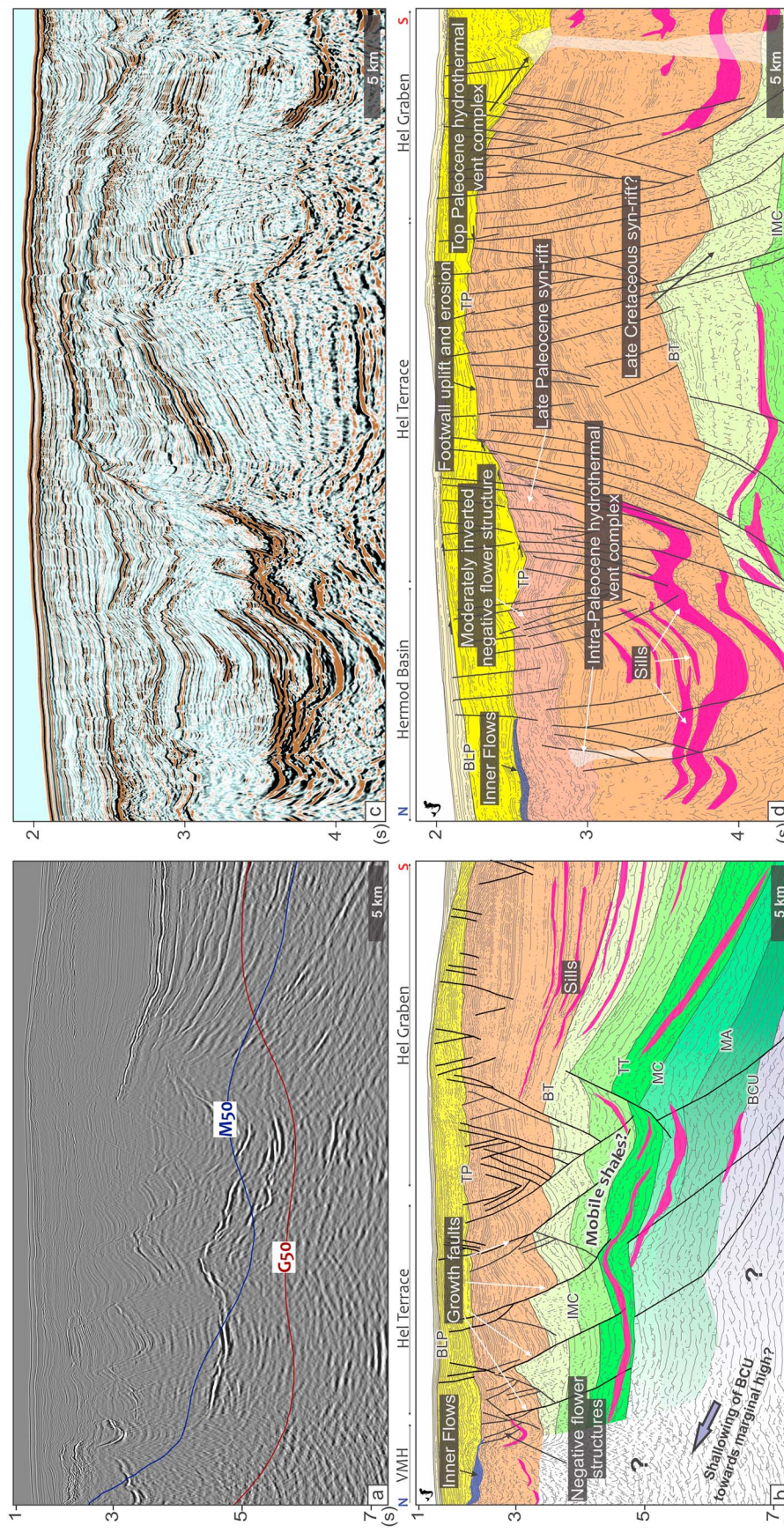


Figure 9. Seismic lines across the Hel Terrace and the Hel Graben. (a) Uninterpreted and (b) interpreted lines: central part of the Hel Terrace with Paleocene rift structures (growth faults) that are controlled at depth by probable lower-mid-Cretaceous mobile shales. Later in the Paleocene, the structure was mildly reactivated in strike-slip regime. The increase of the gravity signal toward the Voring Marginal High could correspond to the shallowing of the BCU level and presence of pre-Cretaceous high/terrace below volcanics. Eastern part of the Hel Terrace: (c) uninterpreted and (d) interpreted lines. Late Cretaceous synrift sequences could develop in the central part of the structure and then superimposed by thick Paleocene sediments related to the collapse of the Hel Graben. Later in the Paleocene, the northern flank of the Hel Terrace was affected by rifting and associated rift-shoulder uplift and erosion. This event was preceded by minor sill intrusions expressed by a venting developed in Paleocene sequences. Major magmatic activity occurred at the Paleocene-Eocene transition with extensive sill intrusions (shown in purple) and development of magmatic sequences at the Voring Marginal High (inner flows). The 50 km high-pass-filtered Bouguer gravity (G50) and magnetic (M50) anomalies are shown for Figure 9a only. The common legend for the sedimentary part is shown in Figure 4. The abbreviations for the horizons are given in section 3.1. The location of the seismic lines is shown in Figure 3.1. Data courtesy of TGS.

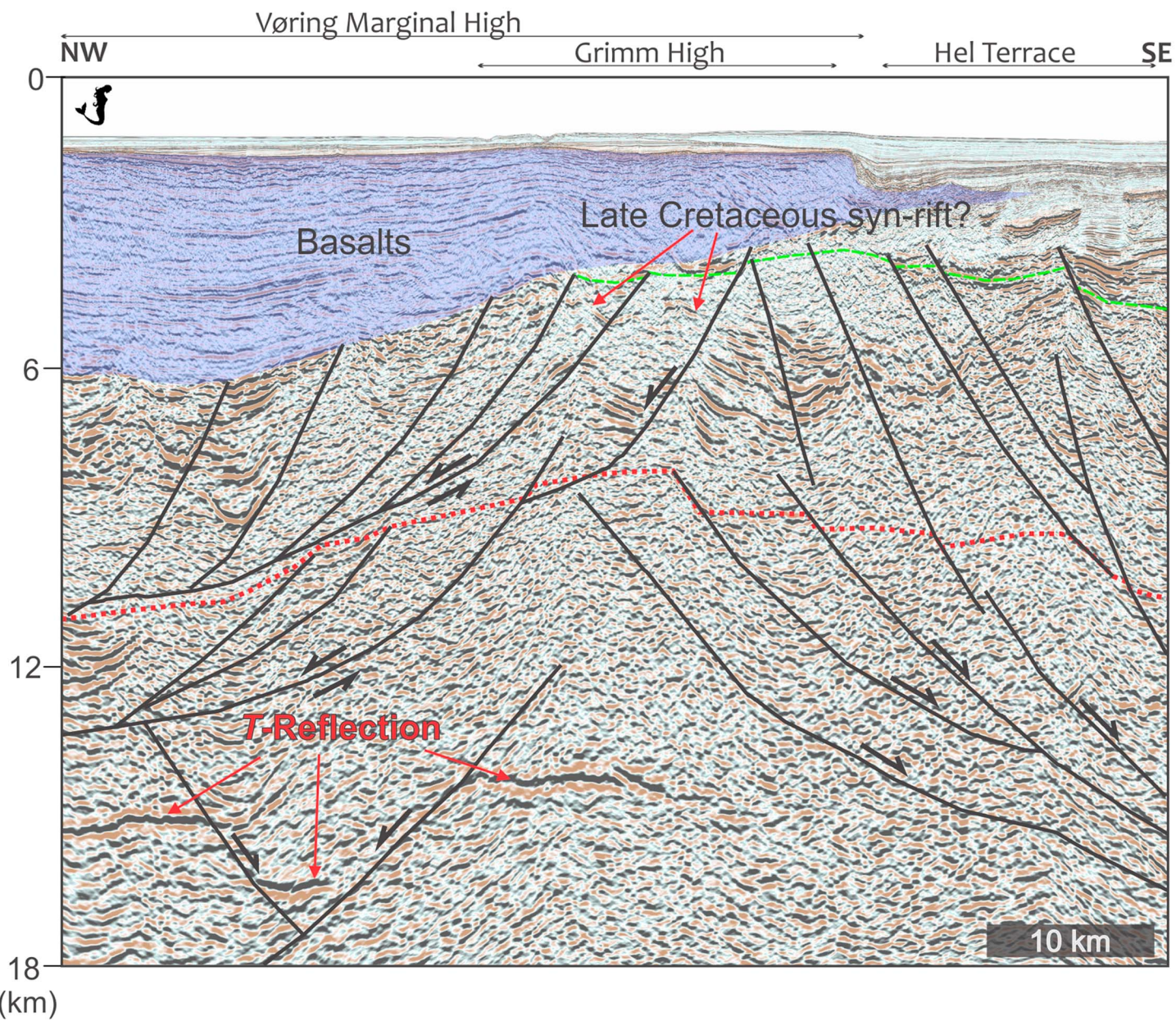


Figure 10. A part of the studied depth-converted transect (see Figure 4a) adjacent to continent-ocean boundary showing subbasalt configuration of the Grimm High. Tilted fault blocks below volcanics could develop within Cretaceous sequences on the analogue with the North Gjallar Ridge (see Gernigon et al., 2003). At about 15 km deep and faulted crustal reflection (*T*-Reflection) is observed. The Base Tertiary and Base Cretaceous Unconformities are shown in dashed green and dotted red, respectively. Data courtesy of TGS.

basaltic cover (Abdelmalak, Planke, et al., 2016), reflecting its relatively high elevation when subaerial volcanic sequences were deposited in the earliest Eocene. Notably, the gravity high observed at that level also fits a high-amplitude reflection observed at 15 km in the deep part of the Grimm High (Figures 4a, 4b, and 10). The deep reflection coincides spatially with the deep and faulted *T*-Reflection described and defined in the outer Vøring Basin (Abdelmalak et al., 2017; Gernigon et al., 2003, 2004). At the level of the Grimm High, the new seismic data revealed tilted fault block system below the volcanics (Figure 10), with a structural style similar to that observed in the adjacent North Gjallar Ridge (Gernigon et al., 2003, 2004; Ren et al., 2003). The upper synrift feature could represent the equivalent of the Campanian-Maastrichtian Springer Formation penetrated by well 6704/12-1 in the North Gjallar Ridge (Fjellanger et al., 2005; Gernigon et al., 2003).

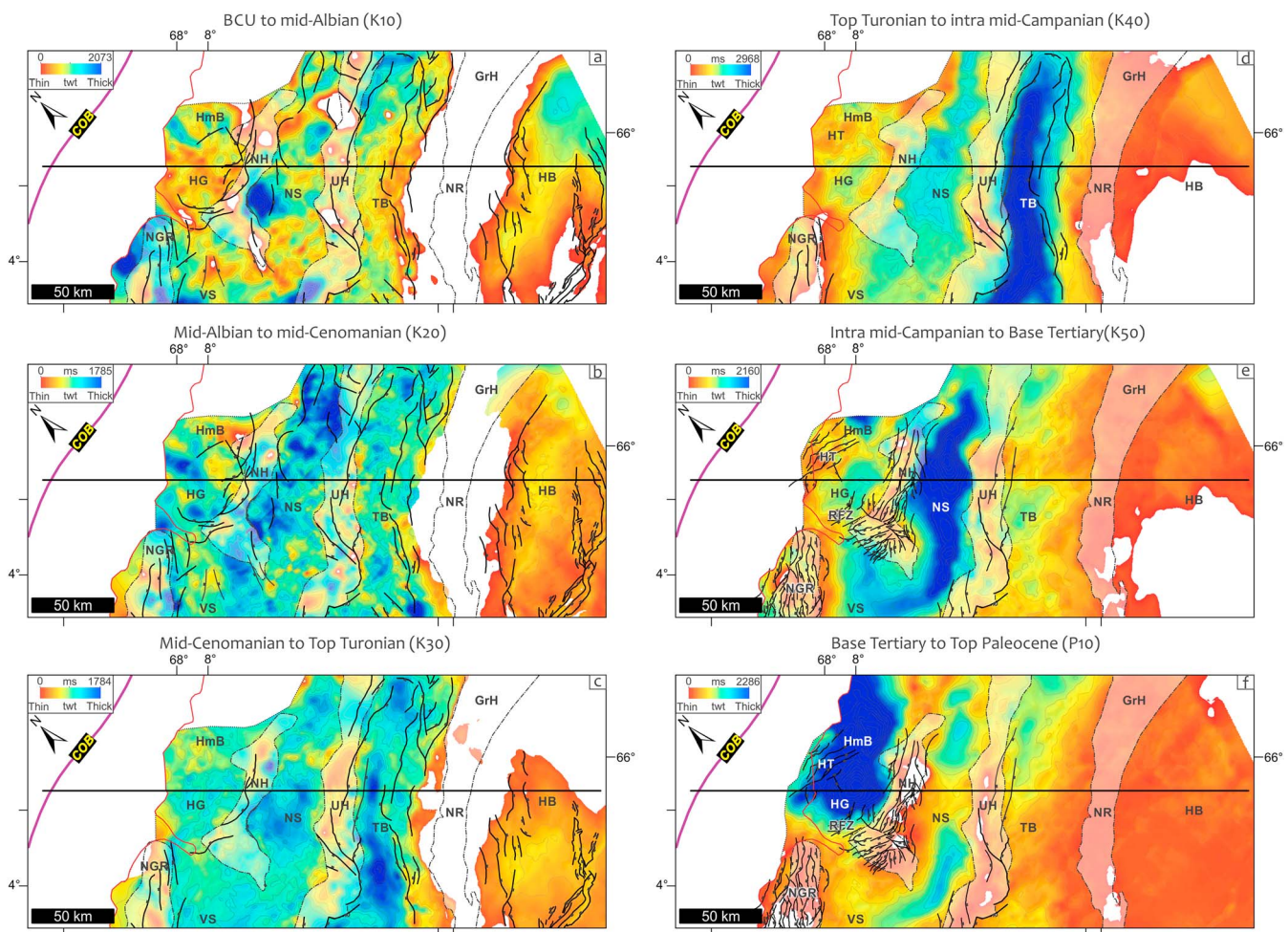


Figure 11. Isochore maps of seismic sequences K10 through P10 showing general distribution and migration of the basin depocenters in time and space. Present structural outline of the main structural highs is shown in transparent white. The red line shows a landward limit of basalt flows. Extent of the maps is shown in Figure 1a. GrH = Grønøy High, HB = Helgeland Basin, HG = Hel Graben, HmB = Hermod Basin, HT = Hel Terrace, NGR = North Gjallar Ridge, NH = Nyk High, NS = Någrind Syncline, RFZ = Rym Fault Zone, TB = Træna Basin, UH = Utgard High, VS = Vigrid Syncline.

4.2. Regional Development of the Main Cretaceous-Paleocene Tectonostratigraphic Units

Having described the present margin geometry, we here infer its evolution based on different isochore maps (Figure 11). We organize this from oldest to youngest, focusing on thickness trends and onlap patterns around major subbasins and flanking structural highs.

4.2.1. Unit K10 (Valanginian to Mid-Albian)

The Valanginian to mid-Albian sequence K10 defined in this study is rather reinterpreted as a synthinning sequence and not a postrift as suggested in previous publications (Færseth & Lien, 2002; Vergara et al., 2001). The isolated rounded depocenter in the Någrind Syncline reflects the Neocomian (Barremian-Aptian?) faulting/rifting activity observed on the eastern flank of the Nyk High (Figures 7 and 11a). However, no prominent and concomitant depocenter is identified within the Træna Basin (Figure 11a). The strata of the K10 sequences onlap the deep terraces imaged in the southern part of the Træna Basin and along the northwestern flank of the Nordland Ridge, which was already an elevated feature at that time (Figure 11a). The uplift of the Nordland Ridge was also associated with lateral subsidence of and sedimentation within the Helgeland Basin, which tends to deepen in the northeastern direction (Figure 11a). As previously interpreted (Blystad et al., 1995; Brekke, 2000), the Lower Cretaceous succession thins toward the Utgard High, suggesting that a local and central horst configuration was already initiated at the early stage of the Vørings Basin formation. Slight thinning and local absence of the K10 sequence on top of the Utgard High is confirmed by our seismic observations (Figures 6 and 11a).

Nevertheless, rather thick Lower Cretaceous sediments are also confirmed by well 6608/2-1S in the northern Utgard High. This reflects a complex structural topography at the early stages of the high formation.

The absence and thinning of the Valanginian to mid-Albian K10 sequence in the southern and central Nyk High suggests NE striking basement/BCU highs, which were already emerged at that time. Several minor depocenters are observed at the transition between the North Træna Basin and the adjacent Lofoten-Vesterålen Margin (Figure 11a).

4.2.2. Unit K20 (Mid-Albian to Mid-Cenomanian).

Similar depositional pattern can be deduced from the mid-Albian to mid-Cenomanian isochore map (unit K20, Figure 11b). Clear erosion is seen on the Nordland Ridge and partly on the deep terraces mapped in the southeastern part of the Træna Basin (Figure 11b). According to the sediment thickness distribution, the Træna Basin was still characterized by a slow sedimentation rate during the K20 deposition. Thinning of the sequence K20 is also interpreted toward the Utgard High (Figure 11b). However, locally poor quality of seismic imaging there makes such interpretation a bit uncertain. We identified several scattered depocenters blanketing the Någrind Syncline and its transition to the Vigrid Syncline and partly the Nyk High (Figure 11b). We also observe significant thickening of the K20 at the transition between the Någrind Syncline and the Lofoten-Vesterålen Margin.

4.2.3. Unit K30 (Mid-Cenomanian-Early Coniacian)

Deposition of the mid-Cenomanian-Early Coniacian unit K30 mainly occurred in the Træna Basin, which defined a deep (up to 1.7 s TWT), prominent and NE-SW elongated (100×25 km), fault-controlled depocenter that deepened toward the southern Rås Basin (Figure 11c). The depocenter-related normal faults tended to develop over older fault systems observed on both flanks of the Træna Basin (Figure 4a). Both seismic observations and isochores indicate that the synthinning subsidence shifted northeastward from the Rås Basin. During the same period, a large and relatively thick rounded depocenter (55×45 km; up to 1–1.5 s TWT thick) developed in the adjacent Någrind Syncline. Thinning of the K30 unit is observed on the SE flank of the North Gjallar Ridge and in the Utgard Ridge, indicating their relatively high structural position during this period (Figure 11c).

4.2.4. Unit K40 (Coniacian to Mid-Campanian)

Rapid subsidence and accommodation of a large, NW-SE elongated (150×30 km) thick depocenter (up to 2.9 s TWT or 6 km thick) during the Coniacian to mid-Campanian K40 period (Figure 11d) concentrated in the Træna Basin. Based on seismic observations, we suggest that fault-driven tectonic subsidence ceased around Santonian and then the Træna Basin was passively infilled during the early to mid-Campanian. Thinning and erosion of the K40 unit on both flanks of the Utgard High confirm its shallow bathymetric configuration at that period (Figure 11d). Rather high sediment accumulation rates persisted along the axis of the Någrind Syncline with the deposition of the Nise Formation sourced from NE Greenland (Morton & Grant, 1998). In the Campanian, the North Gjallar Ridge was still in a relative high position and shallow marine setting as illustrated by the absence and/or pinch out of the K40 unit on its SE flank as confirmed by well 6705/10-1 (Asterix). Furthermore, thinning of the unit K40 toward the Hel Terrace (Figure 11d) also indicates a shallower structure in that domain.

4.2.5. Unit K50 (Mid-Campanian to Base Tertiary)

A dramatic depocenter shift of the unit K50 occurred from the mid-Campanian to the beginning of the Tertiary (e.g., the Base Tertiary Unconformity). The main sedimentation axis moved northwestward from the Træna Basin to the Någrind Syncline (Figure 11e). The depocenter shape mimics the preexisting basin configuration developing in between deep-seated structural highs (Figure 11e). In the SW Någrind Syncline and its transition to the Vigrid Syncline, the depocenter is seemingly not fault controlled. However, subsidence and higher sedimentation in the NE segment of the Någrind Syncline could be enhanced by additional reactivation of the SE dipping faults locally observed on the flank of the adjacent Nyk High (Figure 4a). The sequence K50 is thinned significantly along the Nyk High and the North Gjallar Ridge, which were both uplifted during this period. Smaller thicknesses of K50 are also observed on the Utgard High. Notably, the Hel Terrace was still in a shallower position with K50 onlaps onto its southern flank, suggesting a structural evolution quite similar to the adjacent North Gjallar Ridge.

4.2.6. Unit P10 (Paleocene)

Another marked change in sedimentation pattern happened during deposition of the sequence P10 in the Paleocene, when the depocenter suddenly migrated northwestward toward the Hel Graben and the

Table 1
Density and Magnetic Properties of the Units Modeled in the Present Study

Layers	Density (kg · m ⁻³)	Susceptibility (SI units)	Remanence (A/m)
Water	1,450	0	0
Mid-Pliocene to Holocene	1,800–1,900	0	0
Mid-Miocene to Mid-Pliocene	2,000	0	0
Eocene to Mid-Miocene	2,050	0	0
Basalts/SDR	2,550	0.01	-1 (Upper); +1 (Lower)
Paleocene	2,225	0	0
Intra Mid-Campanian to Maastrichtian	2,400	0	0
Lower Campanian to Intra Mid-Campanian	2,400–2,525 (deep sag)	0	0
Mid-Coniacian to Upper Santonian	2,525–2,575 (deep sag)	0	0
Mid-Cenomanian to Lower Coniacian	2,525–2,600 (deep sag)	0	0
Mid-Albian to Mid-Cenomanian	2,550–2,675 (deep sag)	0	0
Valanginian to Mid-Albian	2,550–2,700 (deep sag)	0	0
Pre-Cretaceous (Und)	2,650–2,775 (deep sag)	0	0
Callovian to Berriasian	2,500	0	0
Toarcian to Bathonian	2,550	0	0
Hettangian to Pliensbachian	2,559	0	0
Upper Triassic	2,575	0	0
Mid-Triassic	2,585	0	0
Mid-Permian to Lower Triassic	2,600	0	0
Upper Devonian?–Permian	2,700	0	0
Upper crust (approximately Caledonian nappes)	2,750	0.01	0
Middle crust	2,850	0.03	0
Lower crust	2,950	0.005	0
High-density lower crust (LCB)	3,100	0.005	0
Ultrahigh density lower crust (ULCB)	3,200	0.015	0
Mantle	3,300 (Lower)–3,250 (Upper)	0	0

Hermod Basin (Figure 11f). In the central part of the outer Vøring Basin, faulting migrated progressively toward the volcanic domain growing at the same period (Gernigon et al., 2004). In the Hel Graben and the Hermod Basin deposition and subsidence were largely controlled by a collapse of the NW flank of the Nyk High and facilitated by a slip along the Rym Fault Zone. Additional evidence for later Paleocene faulting/rifting is seen in the northern part of the basin (e.g., the Hel Terrace) (Figures 9c and 9d).

Minor depocenters in the Vigrid/Någrind syncline axis and near the Lofoten-Vesterålen Margin (Figures 7 and 11f) are not fault controlled; instead, they are likely interpreted as sedimentary bodies (e.g., fans) sourced from the neighboring eroded highs. Erosion of the sequence P10 in the Utgard High is possibly the result of late stages of subsequent Early Tertiary strike-slip reactivation along the Fles Fault Complex as previously noted by Blystad et al. (1995).

4.3. Potential Field Modeling of the Regional Transect and Crustal Configuration

The 2-D forward potential field modeling of the northern Vøring transect (Figures 4a and 4b) was carried out to better constrain the crustal architecture and basement properties underlying the complex depocenter system previously described in this study. The initial crustal parameters used in the potential field modeling are shown in Table 1 (see also Appendix B).

While the Moho configuration in the Trøndelag Platform is constrained by several ESPs (Planke et al., 1991), the depth of top basement was entirely obtained from the new seismic reflection data, where the expected top basement surface represents a well-defined seismic marker. The total crustal thickness decreases down to 10 km in the axial part of the platform, where we have to presume attenuated upper to lower crust and exhumation of the high density, lower crustal body (3,100 kg/m³) at 15 km depth; an interpretation consistent with the high velocities (around 7.1 km/s) and depth estimations was taken from the available ESP data (Planke et al., 1991).

The transition zone to the Træna Basin corresponds to an abrupt thinning of the continental crust over less than 40 km from thickness in 18 km at the Nordland Ridge to 4–5 km in the central axis of the Traena Basin

(Figure 4b). As suggested by Maystrenko et al. (2017), the first necking of the rift system is located in this position. The Moho shallows from 25 km to 20 km in the Utgard-Træna area (Mjelde et al., 1998; Planke et al., 1991).

The northern Utgard High forms the most prominent magnetic and gravity signals along the profile (Figure 4b). In order to fit the prominent gravity signature and surrounding refraction data, we assumed a thick (10–12 km), ultrahigh-density body (ULCB) ($3,200 \text{ kg/m}^3$) from Moho level to relatively shallow position (8–10 km) in the lower and upper parts of the crust. Based on our modeling results, we have to assume 1 km thick midcrustal lenses, which are most likely preserved on both flanks of the structure and almost in contact with the meta-sedimentary prerift and synrift rocks. According to our seismic observations, the top of the ULCB deduced from potential field modeling correlates well with the *UH*-Reflection (Figures 4b and 6) implying a significant impedance (density/velocity) contrast at that level. The basement below the Træna Basin necessitates massive and very high density and magnetic rocks (Figure 4b). Our modeling results do not support the presence and/or preservation of deeper Mesozoic sedimentary rocks in depth. Accordingly, we suppose that the thin and ultrahigh-density lower continental crust may directly underlie the basin possibly coinciding with the strong reflection observed within pre-Cretaceous fault blocks (Figure 5).

A minimum crustal thickness of 5–6 km in the deep-sag Någrind Syncline is expected at the connection to the NW flank of the Utgard High (Figure 4b). The top of the basement is reliably defined in reflection seismic and correlative with refraction data lying at 13 km at the cross point with OBS line 7-96 (Mjelde et al., 1998). The basement shallows to 7.5 km toward the Nyk High and forms a prominent paleohigh with total crustal thickness in 13–15 km also confirmed by OBS line 7-96 (Mjelde et al., 1998) and ESP data (Planke et al., 1991). Lens-shaped bodies of middle, lower crust and a dense LCB (1 to 3 km thick apiece) are required there to fit the observed potential field data.

The axial part of the Hel Graben is not crossed by any refraction profiles (Figures 2b and 4b). We modeled that the Moho rises to 18 km depth, which corresponds to a drastic thinning of the crust reduced to 3–4 km thick in the central part of the Hel Graben. Since we believed that the BCU was confidently interpreted at the position of the transect, we made structural corrections for the pre-Cretaceous configuration in the central Hel Graben (Figure 4a). Based on our modeling, we had to agree on extremely thin or no pre-Cretaceous sediments below this unconformity in order to get a better fit with the observed gravity (Figure 4b). As a result, the Cretaceous sediments most likely lie directly on top of a high-density lower crust also expected in the central part of the Hel Graben (Figure 4b). This crustal configuration also implies that upper to lower crust is most likely substantially delaminated or absent there. The presence of pre-Cretaceous sediments is not totally excluded, but if present, these metamorphosed sequences are extremely compacted and/or highly deformed. With realistic magnetic susceptibility values in the basement, we have not been able to reach a solid fit with the observed magnetic anomalies at the Hel Graben (Figure 4b). This discrepancy could be explained by the magnetic influence of the large shallow sill complex observed in the Hel Graben (e.g., Berndt et al., 2000) but is not considered in our study.

Presence of the deep-seated continental basement block underneath the Vørings Marginal High within the subbasalt Grimm High (Abdelmalak, Planke, et al., 2016) is in agreement with our modeling results (Figure 4b). A crustal fragment with a thickness of more than 10 km is expected there. The Moho beneath the Grimm High is also relatively well constrained at 25 km from previous OBS and ESP data (Mjelde et al., 1997, 1998; Planke et al., 1991) and then shallows to less than 20 km toward the continent-ocean “boundary”. The prolongation of the *T*-Reflection expected at that level partly corresponds to the boundary between the lower crust and the LCB bodies modeled in the distal part of the transect (Figures 4a and 4b). To fit the gravity, our model also suggests that up to 3 km of pre-Cretaceous strata could be preserved above the continental basement expected underneath the basalt.

5. Discussion

5.1. Origin and Geophysical Properties of the Lower Crustal Bodies (LCBs)

5.1.1. Origin of the Utgard Ultrahigh-Density Body (ULCB)

Below the Utgard High our modeling suggests the presence of an up to 12 km thick, ultrahigh-density (3200 kg/m^3) lower crustal body (Figure 4b), the top of which is located almost at the level of the *UH*-Reflection. The shallowing of the *UH*-Reflection in the central and northern parts of the Utgard High fits

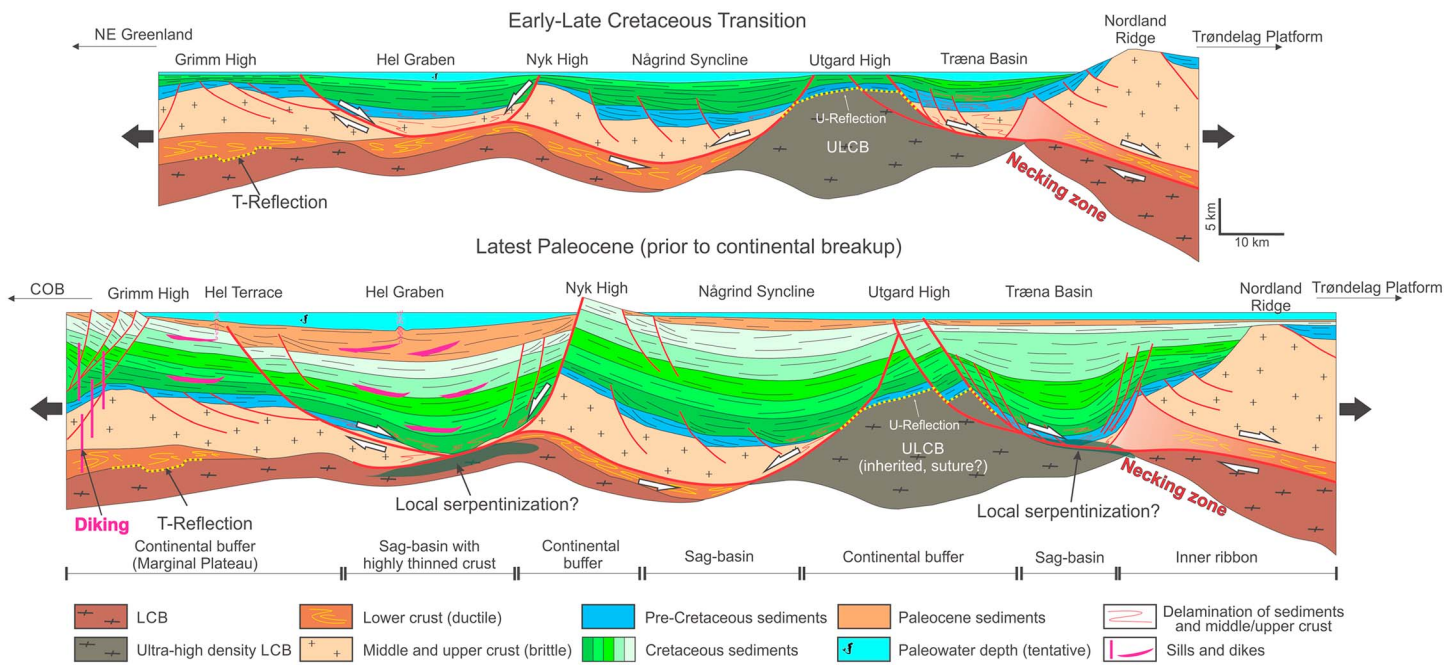


Figure 12. Cartoon illustrating Cretaceous-Paleocene evolution of the northern Vøring Margin.

well with the main magnetic and gravity signals (Figures 6c and 6d). The nature of these potential field anomalies has been extensively discussed. Earlier models (Planke et al., 1991; Skogseid et al., 1992) speculated on the crustal origin of the anomaly, implying that it most likely represents an old, Caledonian, high-density basement block with Mesozoic or pre-Mesozoic age of emplacement. Our observation shows (Figures 6c and 6d) that the *UH*-Reflection corresponds to the top of the local LCB and has been affected by a series of Mesozoic (and older?) faulting events. Consequently, we also considered that the Utgard High LCB (or part of it) is most likely an inherited basement structure.

Mjelde et al. (2013, 2016) also proposed that the basement here partly consists of lower crustal eclogites with a density of up to $3,500 \text{ kg/m}^3$. These eclogites may be related to a sliver of the Caledonian suture zone (e.g., Petersen & Schiffer, 2016). In a recent 3-D lithospheric model of the Lofoten-Vesterålen margin and adjacent parts of the Vøring Margin, a thick high-density lower crustal layer of Caledonian origin, with high densities varying from $2,985 \text{ kg/m}^3$ to $3,070 \text{ kg/m}^3$, has also been considered beneath the Utgard High (Maystrenko et al., 2017).

Reynisson et al. (2010), based on their regional 3-D potential field modeling, interpreted part of the LCB within the Utgard High as heavily (and synrift) serpentized mantle, assuming very thin crust underneath the high. Our modeling and observations suggest, however, that the Utgard High was an old crustal horst partly shielded from drastic thinning (Figures 4 and 12), compared to the surrounding subbasins (e.g., Traena Basin and Någrind Basin). The clear correlation with the central horst system acting as a thick tectonic buffer since the early stage of rifting in the northern Vøring Margin suggests that the high-density rocks were most likely part of the prerift basement even before the onset of drastic thinning of the crust. Wangen et al. (2011) also got unrealistic rates of extension in their tectonic modeling run with a shallow and thin crust at the position of the Utgard High. Therefore, we suggest that the nature of the anomaly is better regarded as a remnant of old Caledonian or Precambrian high-density crustal blocks. Speculative serpentization within the Utgard High is unlikely for us. This system of crustal blocks may extend toward the Lofoten-Vesterålen Margin and merge with either the Lofoten Ridge or the Røst High, which are also expressed as prominent, elongated, positive gravity anomalies. It is likely that the anomaly could also be amplified by significant intrusion of breakup-related, high-velocity, dolerite sills ($>7.0 \text{ km/s}$) as suggested by Berndt et al. (2000) and Neumann et al. (2013). The density expected at the level of the ULCB is so high ($3,200 \text{ kg/cm}^3$) and so massive that we disregarded the possibility of preserved deep sediments at that level. This is in contradiction with recent alternative assumptions from Osmundsen et al. (2016). Shallow magnetic source estimations

(Figure 4b) also support the presence of magnetic (basement) rock at 10–15 km and accordingly cannot easily explain the presence of Mesozoic sediments at that level.

5.1.2. Outer LCB

To fit both the observed gravity and the high velocities also deduced from ESP and OBS data, our modeling also requires a high-density LCB ($3,100 \text{ kg/cm}^3$) in the outer part of the northern Vøring Basin and below the Grimm High (Figure 4b). This body is typically characterized by V_p velocities between 7.1 and 7.7 km/s (Mjelde et al., 2003). The nature of the outer LCB located along continent-ocean boundary has been widely discussed by many authors in the past. Earlier schemes suggest that LCB in the distal part of the mid-Norwegian Margin represented mafic crust underplated during continental breakup (e.g., White & McKenzie, 1989). However, later studies promoted a variety of alternatives on the origin and properties of LCB, ranging from high-velocity intrusions into the lower crust (White et al., 2008, 2010), heavily serpentinized/exhumed mantle (Osmundsen & Ebbing, 2008; Pérön-Pinvidic & Osmundsen, 2016; Ren et al., 1998; Reynisson et al., 2010), and/or a retrograde/high-grade Caledonian lower crust (Abdelmalak et al., 2017; Ebbing et al., 2006; Gernigon et al., 2004; Mjelde et al., 2016; Petersen & Schiffer, 2016).

According to our modeling results (Figure 4b) and new observations (Figure 10), the upper boundary of the outer LCB coincides partly with the subbasalt prolongation of the T-Reflection located at approximately 15 km depth. This high-amplitude reflection also correlates with a strong gravity signal within the Grimm High (Figure 2a). Similar high-amplitude reflection has been earlier described and mapped within the South and North Gjallar Ridges (Gernigon et al., 2003, 2004), where it is also interpreted as a part of an old (possibly Caledonian) inherited piece of lower crust (Ebbing et al., 2006; Gernigon et al., 2004). The T-Reflection influenced the basin evolution long before the onset of the breakup magmatism and as early as the initiation of Late Cretaceous-Paleocene rifting in the mid-Late Campanian (Gernigon et al., 2003, 2004). Furthermore, in the recent study by Abdelmalak et al. (2017), the T-Reflection in the Hel Graben was also interpreted as the top of LCB, where it coincides with lower crustal sill intrusions and detachment faults. An alternative interpretation of the prebreakup emplacement of this LCB may also be explained in terms of serpentinization model in the North Gjallar Ridge (Ren et al., 1998). However, seawater penetration into the mantle could not be easily explained if we consider the thick (8–9 km) prebreakup sedimentary package and the associated decoupled fault system overlying the deep LCB (Figure 10). Thus, in our model we agree that an inherited crustal origin of the LCB is most likely for this distal part of the margin.

5.2. Basin Evolution and Crustal Deformation

5.2.1. Træna Basin Revisited: Too Narrow and Deep To Be Just a Postrift Cretaceous Sag Basin?

Very few papers have described the Træna Basin in detail (Blystad et al., 1995; Gomez et al., 2004; Osmundsen et al., 2002). According to Osmundsen et al. (2002), the Træna Basin represents a large rollover structure controlled by an east dipping detachment fault along the southeast side of the Utgard High, which influenced the subsidence of the basin and the formation of two large Lower and Upper Cretaceous depocenters. In contrast, Gomez et al. (2004) proposed that the Træna Basin was rather controlled by a large west dipping detachment fault defining the NW flank of the Nordland Ridge, whereas the NW dipping flexure of the Nordland Ridge was explained by Late Cretaceous, postrift thermal subsidence. We do not see any evidence for a significant west dipping detachment faulting at the BCU or deeper level along the flank of the Nordland Ridge and its transition to the Træna Basin. The Træna Basin could be initiated as a half-graben on the flank of the Utgard High in the Jurassic-Early Cretaceous, with the Nordland Ridge being uplifted and peneplaned (Blystad et al., 1995; Brekke & Riis, 1987) as a flexural response during this rifting event, as later proposed by Osmundsen et al. (2002). According to our observations, the subsequent formation of the elongate, narrow, and extremely thick Upper Cretaceous depocenter of the Træna Basin is fault controlled on both sides of the basin but is not only structurally limited to the southeastern side of the Utgard High. Therefore, the existence of an active and persistent west dipping detachment through the entire thinning history of the Træna Basin is questionable.

The conjugate fault systems observed on both sides of the Træna Basin (Figure 4a) are sealed by Santonian strata and then were moderately reactivated mainly along the Utgard High as a continuation of the Fles Fault Complex in latest Cretaceous-Paleocene times. One could explain this faulting as a simple result of differential compaction during a long period of postrift thermal sagging of the basin (Færseth & Lien, 2002). However, the backstripped tectonic subsidence curve (Figure 13) calculated for the central part of the Træna Basin shows

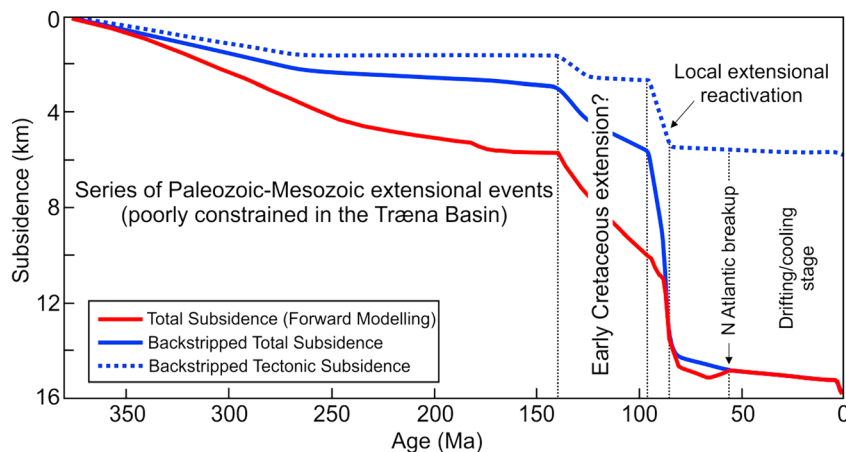


Figure 13. Total and tectonic subsidence curves calculated by different methods (forward modeling and backstripping) on the axial part of the Træna Basin. Extreme subsidence rates obtained for mid-Cenomanian-Santonian time are typical for strike-slip related basins and also can be attributed to rift basins associated with steep-dipping faults. Subsidence curves were computed using the TecMod 2-D software.

an abrupt transition to relatively rapid subsidence magnitude (~2.5 km) starting in the mid-Cenomanian (~95 Ma) and ceasing at Santonian (~85 Ma). Such rapid subsidence (Figure 13), the atypical high rates of sedimentation during this geologically short time period (10 Myr), and the narrow basin configuration (~20 km wide) cannot be easily explained by a McKenzie-like thermal subsidence model (McKenzie, 1978) invoking uniform and instantaneous pure shear extension. Narrow, small basins characterized by accelerated and short-lived tectonic subsidence (2–4 km in 10 Myr) typically form in pull-apart settings, where transtensional strike-slip regime is involved (Christie-Blick & Biddle, 1985; Xie & Heller, 2009). Typical strike-slip basins (e.g., Dead Sea Rift (ten Brink & Ben-Avraham, 1989)) tend to lengthen rather than widen during ongoing extension. Transtensional regimes also favor much faster and efficient thinning of the crust, which seems to be the case in the Træna Basin according to the very thin crust expected there (Figure 4b). Notably, Early to Late Cretaceous oblique extension and dextral strike slip have been described in the adjacent Lofoten-Vesterålen Margin (Bergh et al., 2007).

The observed fault systems controlling the mid-Cenomanian-Santonian subsidence in the Træna Basin show relatively steep configuration (Figure 4a). However, direct evidence for both large-scale strike-slip motions (e.g., negative flower structures) is not well imaged along the basin. Furthermore, the backstripped tectonic subsidence rate in 2.5 km is not uncommon for rift basins (Allen & Allen, 2013). The formation of steep-dipping faults in a narrow rift basin could explain ongoing rapid subsidence even after rift opening had slowed, as is shown in the Rio Grande Rift (van Wijk et al., 2018). In this case, local transtensional reactivation or extension by slip on steep-dipping faults could explain the mid-Cenomanian-Santonian structural evolution of the narrow, deep Træna Basin. Unfortunately, our observations and modeling results cannot fully discriminate between the two scenarios. Nonetheless, a local extensional component during the Cenomanian-Santonian thinning of the Træna Basin could be concomitant with the uplift and tilting of the Trøndelag Platform (Brekke, 2000), the Nordland Ridge (Fjellanger et al., 2005), the Lofoten Margin (Henstra et al., 2016), and the Utgard High. Our biostratigraphic study of well 6608/2-1S in the northern Utgard High (see appendix and Figure A1 for details) reveals the presence of a significant Turonian hiatus that could be a result of vertical movements linked with this possible thinning event. Mid-Coniacian extensional reactivation along the flanks of the Træna Basin was also assumed in the regional paleobathymetric model by Roberts et al. (2009). However, the authors did not provide any structural examples for that.

In previous publications, the Træna Basin was characterized by a thick (2 s TWT) Lower Cretaceous succession and the Base Cretaceous Unconformity lying at approximately 6–7 s TWT (Blystad et al., 1995), shallowing toward the Lofoten-Vesterålen Margin. In previous study, Osmundsen et al. (2002) interpreted the BCU at a deeper level (8 s TWT) but also presumed a thick Lower Cretaceous succession (up to 3 s thick TWT). Our interpretation and regional seismic tie consider thinner Lower Cretaceous sediments in the Træna Basin (Figures 4a, 5, and 11a). The absence of thick Lower Cretaceous depocenters in the Træna Basin is also in

contrast to Vergara et al. (2001), who proposed regional sediment passive infill of inherited rift-related Jurassic lows during the Berriasian to Albian. On the one hand, the Træna Basin could have been a sediment-starved unfilled rift system at this time. However, relatively thick Lower Cretaceous strata are also preserved on top of the Utgard High “crustal buffer” (Figure 6d), which was located in a shallower position at that stage (Figure 11a). Accordingly, we speculate that much thicker Early Cretaceous sediments would have most likely coexisted in the adjacent subbasin. To explain such an ambiguity, we propose a crustal scenario where pre-Cretaceous and partly pre-mid-Albian successions were most likely deposited in the proto-Træna Basin but were subsequently drastically stretched during the Late Jurassic-Cretaceous extensional events (Figure 12). Such a mechanism was described onshore in the inverted Northeastern Pyrenean rifted margin (Clerc et al., 2015, 2016), where similar synrift basins developed over greatly thinned continental crust with basin floors representing locally exhumed continental lower crust. In such drastic thinning environments, Clerc et al. (2016) show that both prerift and synrift sediments can be affected by synmetamorphic ductile deformation and transported/delaminated together with the extended and highly thinned continental crust. This field analogue could most likely apply to the Træna Basin, where the potential field modeling also supports a drastic thinning of the crust just underneath the Cretaceous sediments (Figures 4b and 12). The thinned continental crust in the Træna Basin predominantly consists of ultrahigh dense material of possibly Caledonian and/or older origin. This crustal body extends and thickens northwestward in the prolongation of the seismic and structural grain observed in the deep basement part of the Utgard High. We propose that the upper-middle crust with prerift and synrift sediments were deformed and largely squeezed and delaminated in the central part of the Træna Basin, during the exhumation of an old lower crust which are almost in contact with the synsag sediments. Due to the great depth of the sediments observed in the Træna Basin, metamorphism and associated ductile deformation is a reasonable hypothesis to propose. It may also explain the difficulty to image any consistent seismic packages underneath the BCU. After Late Jurassic-Early Cretaceous rifting, another active phase of crustal thinning renewed in the Træna Basin and adjacent areas during the mid-Cenomanian-Santonian. This could explain the sudden increase of the subsidence rate suggested by Figure 13.

5.2.2. Deformation Patterns in the Nyk-Någrind Segment and the Hel Graben

Thanks to the new TGS data, we see clear evidence for a separate Neocomian (Barremian-Aptian?) rifting between the Någrind Syncline and the Nyk High (Figures 7 and 11a). This event succeeds the Jurassic-earliest Cretaceous extensional phase particularly well recognized and constrained in the platform area (Blystad et al., 1995; Brekke, 2000). Up to the mid-Cenomanian, post rift mainly concentrated within the basin low created during the Late Jurassic-Neocomian (Barremian-Aptian?) extension. From the mid-Cenomanian to Campanian, both increasing subsidence and deposition shifted southeastward (Figures 11b and 11c). The depocenters appear to be partly controlled by a west dipping detachment fault along the adjacent flank of the Utgard High (Figures 4a and 4b). This observation is partly in agreement with Skogseid et al. (1992), who speculated earlier on a similar development of the Utgard High and its surrounding basins. The middle crust and possible pre-Cretaceous prerift/synrift sediments in the adjunction to the Utgard High are drastically stretched along the detachment, with the total crustal thickness of 5–6 km (Figure 4b) constrained by our 2-D potential field modeling and also in agreement with Maystrenko et al. (2017).

Previous studies (Brekke, 2000; Lundin et al., 2013; Lundin & Doré, 2011) suggest that the folded geometry of the Någrind Syncline is not a result of a thermal subsidence following the Jurassic-Early Cretaceous rifting phase (Doré et al., 1999) but the consequence of a large-scale lithospheric folding caused by a modest Maastrichtian regional compression (Bjørnseth et al., 1997; Lundin et al., 2013). Parallel-bedded strata with relatively uniform thickness below the syncline could support this interpretation (Bjørnseth et al., 1997). However, we argue that after initial subsidence caused by a series of Late Jurassic to Neocomian extensional events, the Någrind Syncline had a “steer’s head” basin geometry with slightly increased sedimentation in its central part and sediment thinning toward the adjacent Nyk and Utgard Highs (Figure 11). Such a geometry is typical for basins that experienced thermal subsidence after a stretching episode (White & McKenzie, 1988). Subsequent reshaping of the Någrind Syncline occurred in mid-Campanian-Maastrichtian time, when the rift axis jumped toward the Hel Graben (Figures 11e and 11f). During this renewed activity, the northwest flank of the Nyk High started to rise and fault as a rift shoulder. The uplift of the Nyk High (Figures 4a, 5, 11e, 11f, and 12) generated a concomitant tectonic flexure and rapid subsidence in the Någrind Syncline leading to the formation of a deep depocenter (Figure 11e). We, therefore, prefer to attribute the present-day geometry

of the Någrind Syncline to extensional processes rather than a compressional buckling as proposed by Lundin et al. (2013).

Furthermore, in the outer Vøring Basin clear extension dominated in the North and South Gjallar Ridges since the mid-Campanian (Gernigon et al., 2003; Ren et al., 2003). This late rifting event is associated with the formation of clear and prominent synrift wedges (Springar Formation) and normal faults partly cut by the Base Tertiary unconformity (Gernigon et al., 2004). We also precise that the presence of a shallowing Turonian (Lysing Formation) across the North Gjallar Ridge and the Fenris Graben (Osmundsen et al., 2002) is not any longer valid since well 6704/12-1 confirms that these synrift sediments are dominantly Campanian-Paleocene in age. In contrast to Lundin et al. (2013), we also believe that the main extension phase in the Gjallar Ridge initiated in the mid-Campanian and not Paleocene, where most of the deformation already migrated toward the volcanic province. In the adjacent Vigrid Syncline, as suggested by Kjennerud and Vergara (2005), an increased sedimentation in the mid-Campanian-Maastrichtian could also be a response to the onset of this rifting phase in the outer Vøring Basin.

Our study shows that the subbasaltic Grimm High resembles the North Gjallar Ridge. In addition to the faulting shape of the T-Reflection, we also define about 8–10 km of possible pre-Cenozoic rocks capping the reflection (Figure 10), although poorer seismic imaging below volcanics does not allow a more confident interpretation. Similar structural styles (i.e., tilted fault blocks within Cretaceous strata) and nearly synchronous vertical movements within the Grimm High area and the North Gjallar Ridge during Turonian to Maastrichtian times (Figures 3, 11d, and 11e) suggest that they might be parts of the common structural domain at this time.

The nature of the sudden Paleocene collapse of the Hel Graben is still debatable (Lundin et al., 2013). It is clearly associated with the Nyk High hanging wall slipping toward the graben center, but the crustal mechanism responsible for the structure formation remains unclear. Lundin et al. (2002) proposed that the Hel Graben was formed by a Paleocene caldera eruption possibly coeval with igneous activity associated with the extensive intrusion of high-velocity sills, which thus might have taken place prior to breakup time (Berndt et al., 2000). Evidence for older intra-Paleocene sill intrusions is observed in the Hel Graben (Figure 9b) and could support this interpretation, but the size and origin of such a putative caldera remain difficult to explain. Another model (Gernigon et al., 2003) assumed that breakup-related magmatism and thinning could provoke lateral flow of a ductile lower crust below the rift zone. This model could similarly explain both Paleocene uplift of the Nyk High and the collapse of the Hel Graben. Later, Lundin et al. (2013) proposed several other possibilities including similar crustal delamination and magma withdrawal during chamber deflation (e.g., Pinel & Jaupart, 2005).

Our seismic interpretation and modeling results consider a highly thinned crust (<5 km) below the Cretaceous-Paleocene Hel Graben (Figures 4b and 4c). We can only restore and constrain evidence of Late Cretaceous to Late Paleocene rifting/faulting in the Hel Graben and surrounding structures. However, it is possible that the deepest and older Cretaceous sediments rest directly upon the LCB (Figures 4b and 4c), while middle-upper crust and pre-Cretaceous prerift/synrift deposits (if they still exist) were totally delaminated and/or boudined in the similar mode previously described in the Traena Basin (Figure 12). Such crustal removal could be largely controlled by a detachment faulting system observed along the western flank of the Nyk High and possibly on the eastern flank of the Grimm High/Hel Terrace lying on the conjugate side of the expected Paleocene rift/thinning axis (Figures 4b and 4c). Together with the breakup-related magmatism, this thinning event could have promoted a collapse of the Hel Graben and uplift of the Nyk High as proposed in the model of Gernigon et al. (2003). Depositional patterns and the rapid Paleocene subsidence rates may indicate that the main phase of thinning took place during the Paleocene rifting phase restricted to the Hel Graben and possibly underneath the basalt in the central outer part of the Vøring Margin (e.g., the Fenris Graben). Poorer seismic imaging at greater depth in the area makes hard to estimate the amount of crustal thinning in the earlier rifting phases. The possible presence of pre-Cretaceous sediments at the Grimm and Nyk highs (Figures 4a and 4b) allows us to speculate that the pre-Cretaceous basin on top of the thinned crust could also coexist within the Hel Graben, although appropriate sediments could be highly metamorphosed and delaminated at least during Late Cretaceous-Paleocene rifting and likely during earlier extensional phases.

Compared to the Hel Graben, the crustal blocks preserved on the flanks (e.g., the Grimm High and Nyk High) show evidence of thicker continental crust (Figure 4b), less affected by the Paleocene thinning compared to the adjacent Hel Graben. We interpret this specific crustal configuration in terms of boudinage of the crust (Figure 12) (see Gartrell, 1997) which appears to be a key process in many other rifted margins worldwide (Clerc et al., 2017). The Nyk and Grimm Highs most likely represent thick crustal swell or boudin in between the subbasin (Hel Graben), where drastic thinning deformations were localized (Figure 12).

It is also important to note that the Hel Graben experienced a different tectonic history compared to the other segments of the outer Vøring Basin. Increasing faulting events and drastic Paleocene sedimentation in the Hel Graben (Figure 11f) are synchronous to uplift and progressive decrease of the normal faulting observed farther south in the central segment of the outer Vøring Basin (e.g., North and South Gjallar Ridges). We propose that this difference is possibly linked with the localization and migration of the deformation during the Paleocene. The crustal thinning estimation suggests that in the Paleocene, the Hel Graben was almost close to the breakup stage if we assume a crustal thickness of less than 4 km (Figures 4b and 4c). However, the breakup finally occurred 65 km farther west. It suggests that the Paleocene rift axis that almost dissected the Hel Graben failed to propagate farther south and jumped west of the Grimm High during the earliest Eocene breakup. The final jump is possibly explained by the onset of magmatism (Figure 12), likely leading to extra weakening and rift localization in the western branch of this complex overlapping system. Similar processes of rift migration/abortion triggered by magmatism and underplating are described in Yamasaki and Gernigon (2010).

5.3. Regional and Generic Implications

5.3.1. Early (Neocomian) and Mid-Cretaceous Extension in Its Regional Context

We may identify evidence for significant Cretaceous tectonic activity in the northern Vøring Margin. While Late Jurassic-Early Cretaceous and Late Cretaceous-Paleocene extensional phases are widely accepted and confirmed by structural observations and drilling, Neocomian and mid-Cretaceous (Aptian to nearly Campanian) rifting events are often neglected, rather ambiguous, and often interpreted as a passive sedimentary infill during postrift thermal subsidence (Færseth, 2012; Færseth & Lien, 2002; Skogseid et al., 2000). Recent drilling results from the Vøring Basin; for example, well 6603/5-1 at the South Gjallar Ridge and well 6608/2-1S at the Utgard High (NPD factpages, 2017) proved much thicker Lower and Upper Cretaceous sediments than previously believed (Blystad et al., 1995; Skogseid et al., 2000; Swiecicki et al., 1998). Such misinterpretation in the proposed stratigraphy is primarily the results of previous underestimation of the sedimentation rates throughout the Cretaceous period and consequently may explain the minimization of the mid-Cretaceous extension (Færseth & Lien, 2002). However, previous evidence for prominent early-to mid-Cretaceous extensional tectonism has been reported in the Rå and Gjallar Ridges in the outer Vøring Basin (Gernigon et al., 2003), the Lofoten-Vesterålen Margin (Henstra et al., 2016; Tsikalas et al., 2001, 2005), the Någrind Syncline, and the Træna Basin (Figures 7 and 12; this study). Aptian-Cenomanian extension at the southern end of the Nordland Ridge was also suggested by Pascoe et al. (1999). It is not impossible that this extensional deformation may have propagated north, along the flank of the Nordland Ridge, triggering mid-Cenomanian-Santonian extensional reactivation in the Træna Basin. Activation of the Nordland Ridge as a sand source in the Cenomanian and Turonian-Coniacian (Lysing Formation) was also suggested by Doré et al. (1999) and Fjellanger et al. (2005). Furthermore, coeval tectonic reactivation was observed along the onshore continuation of the Møre-Trøndelag Fault Complex (Sømme & Jackson, 2013). Nearly coeval apatite fission track ages (since 100 Ma) of fault reactivation and block uplift of kilometers scale within the Møre-Trøndelag Fault Complex have been reported from the Norwegian mainland (Redfield et al., 2005). Beyond that, in the wider North Atlantic realm, we have well-documented evidence of Early to mid-Cretaceous extension, including Aptian rifting in the SW Barents Sea (Faleide et al., 1993; Serck et al., 2017), mid-Albian faulting activity in the NE Greenland (Whitham et al., 1999), and Berriasian to Cenomanian synrift deposition in the Rockall Trough (Corfield et al., 1999). The prominent Late Mesozoic rifting phases in the Faeroe-Shetland Basin likely occurred in the Neocomian, Aptio-Albian, Cenomanian-Santonian, and Campanian-Maastrichtian (Dean et al., 1999), whereas minor Turonian-Coniacian fault reactivation in the region promoted coeval sand deposition identical to the Lysing Formation in the Norwegian Sea (Grant et al., 1999). All above mentioned structural observations make it likely that the entire mid-Norwegian Margin and the northern Vøring Margin segment, in particular, were subjected to similar early to mid-Cretaceous events in the regional context contrary to the quiescence

interpretation of Færseth and Lien (2002). These events were possibly not associated with a prominent and continuous rifting axis in the mid-Norwegian Margin but represented scattered, isolated, and migrating rifting centers that were selectively reactivated along basement highs and old mobile zones (Lofoten Ridge, Nordland Ridge, Nyk High, Surt Lineament, Jan Mayen Corridor, etc.).

5.3.2. On the Role of Crustal Inheritance in the Margin Development and the Presence of Serpentinized Mantle in the Vøring Basin

As mentioned above, recent tectonic models suggested the presence of a partially to heavily serpentinized mantle in the Vøring Basin (Péron-Pinvidic et al., 2013; Péron-Pinvidic & Osmundsen, 2016; Reynisson et al., 2010; Rüpke et al., 2013). Extremely thinned crust in the Hel Graben and the Træna Basin (Figure 4b) could favor such tectonic scenario there. Pérez-Gussinyé and Reston (2001) suggested that serpentinization can be likely achieved in the settings with thinning (β) factors above 3 and a crustal thickness less than 8 km. However, in addition, we have to consider the timing and duration of the main thinning phases, decompacted sediment thicknesses during these phases, and the development of basin-scale faults in order to understand environments that could promote or block water passage to the mantle and lead to a partial serpentinization. All these parameters should be then estimated, integrated, and tested within different modeling approaches to allow testing of various hypotheses. However, our tectonic model also supports the early presence of inherited continental crust and related LCB over most of the highs observed in the Vøring Basin (Figure 12). It is unlikely that a broad zone of exhumed mantle affected the entire Vøring Basin, and the presence of exhumed mantle underneath the basalt cannot explain the shallow environments suggested by new seismic interpretation and petrology derived from the ODP drilling in the Vøring Marginal High (Abdelmalak, Meyer, et al., 2016; Abdelmalak, Planke, et al., 2016). If serpentinization occurs, it would eventually be restricted to local windows in the deepest part of the subsag basins involved in this boudined and mullioned type of superextension (Figure 12). Other observations from worldwide rifted margins (Clerc et al., 2017) and also various numerical models also support the presence and persistence of inherited crust underneath similarly large sag basins (Brune et al., 2014; Petersen & Schiffer, 2016).

The presence of older crustal grains and crustal weakness zones has a significant influence on basin development and architecture. While analogue and numerical models deal mostly with homogenous and uniform mode of extension in the rifted margins (Lavier & Manatschal, 2006), crustal inheritance and late magmatism could explain complex geometries and deformation migration and localization discussed in this paper. The inherited crustal blocks and associated structures/fabrics initiate and control the onset and development of thinning deformations of the continental crust (Abdelmalak et al., 2017). This “boudinage style of deformation” is similar to what has been previously described and proposed by Lister et al. (1986), Gartrell (1997), or Clerc et al. (2017). For the Northern Vøring and Lofoten-Vesterålen Margins, such a tectonic scenario was proposed almost 30 years ago by Anderson (1986) who, based on gravity anomalies analysis, suggested the existence of large-scale boudinage of the continental crust which makes up the margin. Furthermore, these weakness zones could be associated with major lithosphere structural discontinuities (e.g., sutures and mega-shear zones). Their orientation and deformational pattern could give us better constraints in paleore-contractions and better understand their role in the margin segmentation. Similar tectonic regimes occurred in the development of other rifted margins (Chian et al., 2001; Clerc et al., 2017; Franke et al., 2014; Funck et al., 2008; Gernigon et al., 2014; Sun et al., 2009). Therefore, we caution researchers to apply “classical” hyperextended Iberian scenarios in complex tectonic settings such as the mid-Norwegian Margin. In the mid-Norwegian Margin larger and thicker continental crustal masses with rather complex petrophysical properties and spatial distribution are involved. Its rift development is also polyphase and shows a much longer period of episodic rifting event compared to the Iberian rifted margin types.

6. Conclusions

1. We investigated and interpreted new seismic data in the northern Vøring Margin poorly constrained by deep seismic data in the past. Combined with regional map production and potential field modeling, we propose a new tectonic scenario for the mid-Norwegian Margin.
2. We argue that the northern Vøring Margin and the entire mid-Norwegian Margin were tectonically active during mid-Cretaceous in contrast to Færseth and Lien (2002). We found seismic evidence of Barremian-Aptian (?) faulting activity in the Någrind Syncline and mid-Cenomanian-Santonian extensional

reactivation in the Træna Basin. This may indicate a nonuniform and nonlinear distribution of rifting centers in the Early to mid-Cretaceous within the Vørting Margin likely reflecting selective tectonic reactivations along preexisting mobile zones.

3. The Træna Basin is a narrow basin with a thin crust (4–5 km) which initiated since the Late Jurassic as a half-graben developed on the flank of the Utgard High. Possible later mid-Cenomanian-Santonian extensional reactivation significantly increased the basin subsidence and the thinning of the underlying continental crust. Presynrift and partly synrift sediments together with upper-middle crustal rocks at the basin floor might have been significantly deformed and delaminated/compacted during these extensional phases
4. According to our observations and modeling results, the crust underneath the Utgard High likely represents ultrahigh-density body ($3,200 \text{ kg/m}^3$) of Caledonian or older (Precambrian) origin. The top of this body corresponds to the strong *UH*-Reflection. Detachment faults developed on the flanks of this rigid continental block and controlled the prethinning and synthinning Mesozoic evolution of the adjacent basins (e.g., the Någrind Syncline and the Træna Basin).
5. We see no prerequisites to explain the configuration of the Någrind Syncline as a result of compressional buckling as previously suggested by Lundin et al. (2013). Our analysis shows that the Någrind Syncline has been formed by a migrating sequence of extensional and postextensional events and associated vertical movements from the Early Cretaceous to the Early Eocene.
6. The Hel Graben is a deep Cretaceous-Paleocene basin that developed in between two rigid block ("continental buffers"). The thinning deformation in the Hel Graben was controlled by detachments on the flanks of these blocks (the Grimm High and the Nyk High) with a culmination in the Paleocene that led to a collapse of the structure. We suggest very thin upper and middle crustal rocks and prerift and synrift sediments in the axial part of the Hel Graben. They are most likely highly deformed and metamorphosed along detachments. Extremely thinned crust (3–4 km) indicates that the Hel Graben was very close to the breakup stage in the Paleocene until the rifting axes eventually jumped in the late Paleocene-earliest Eocene toward the present continent-ocean "boundary". We also found evidence of intra-Paleocene intrusive magmatism preceding the main magmatic event during the earliest Eocene continental breakup.
7. The *T*-Reflection observed underneath the North Gjallar Ridge extends toward the Grimm High and might be of the same origin, that is, old inherited Caledonian lower crust. These structures could be part of a common structural trend before the Paleocene extensional phase.
8. We do not expect wide zones of mantle exhumation and serpentization in the Vørting Basin; however, local areas of serpentization could eventually develop in deep subbasins with significantly thinned crust (Træna Basin and Hel Graben). Nonetheless, in our opinion, the mid-Norwegian Margin represents a unique type of a volcanic rifted margin, where large inherited crustal blocks define a long and polyphase development and a complex deformation distribution. Combined with the presence of SDRs along the continent-ocean transition, it has very little in common with the Iberian nonvolcanic rifted margin types.

Appendix A: Stratigraphic Comment on Well 6608/2-1S, Utgard High

This appendix provides a detailed stratigraphic comment on the selected Cretaceous intervals and log pattern interpretation of well 6608/2-1S. The well 6608/2-1S has been analyzed by RPS Ichron. The raw results of biostratigraphic analyses and wireline logs have been provided by the Norwegian Petroleum Directorate (NPD) via the Diskos National Data Repository. After review and integration, these data formed the basis of stratigraphic interpretation.

A1. Early Cretaceous Intervals

The Early Cretaceous interval is dated in both the main hole and ST2 bypass where the sidewall core samples have been analyzed providing stronger age confidence (Figure A1).

The top of the Langebarn Formation is defined with the use of the change in the log pattern and is supported with the presence of *Caudammina ovula crassa* foraminifera (Figure A1). The Albian interval of the formation is characterized with the sparse palynological assemblage, consistent with the interpretation, with rare presence of *Batioladinium micropodium*, *Muderongia asymmetrica*, and taxa of a broad Early Cretaceous range. The presence of *Aptea polymorpha* is considered to be characteristic of the Albian period in the northern latitudes (Nøhr-Hansen, 1993).

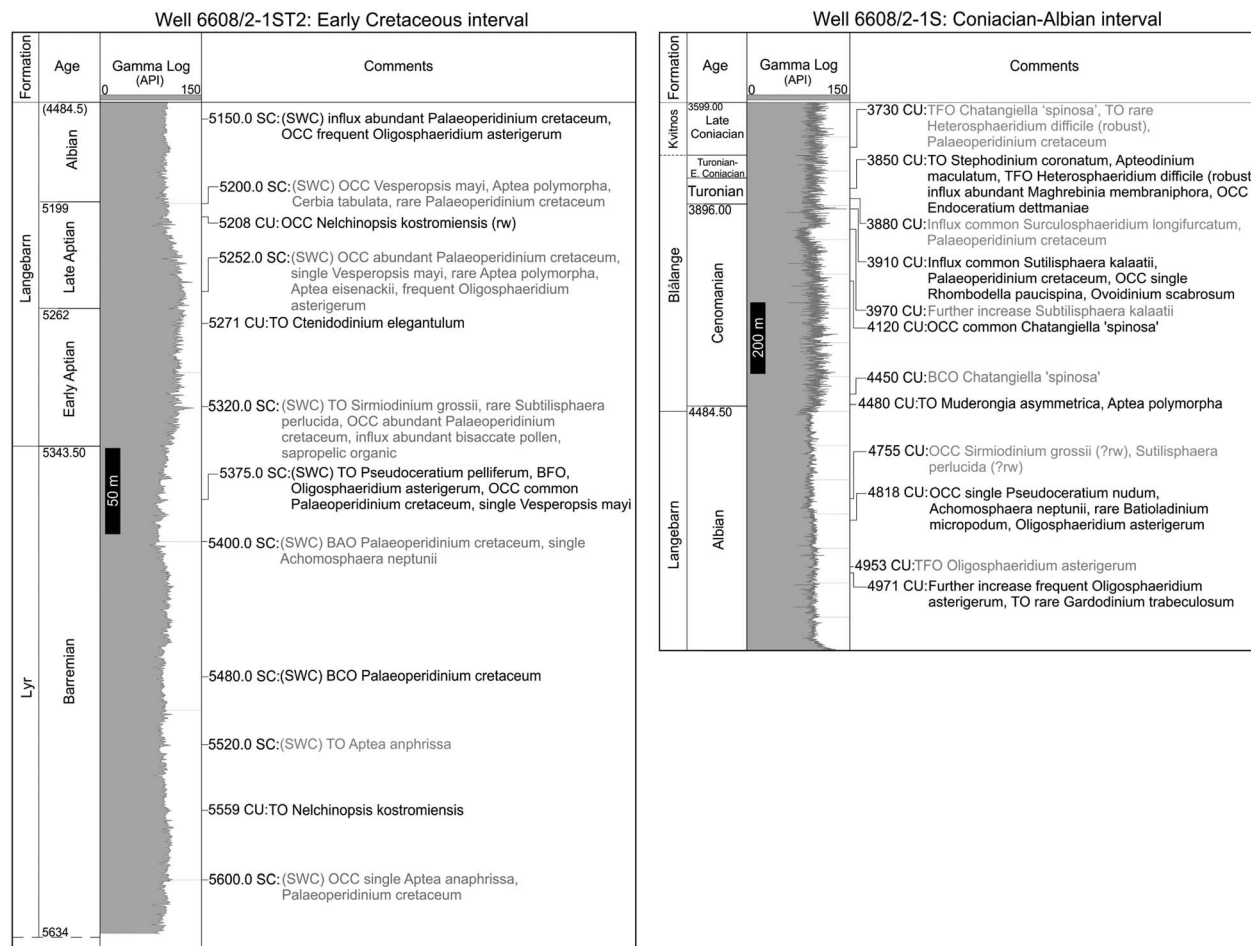


Figure A1. Well 6608/2-1S and ST2 bypass. Biostratigraphy summary chart of Barremian to Coniacian intervals. Formation names after NORLEX (Gradstein et al., 2010).

The Late Aptian section of the well is characterized by the prominent gamma log pattern (Figure A1), suggesting the paleoenvironments with the decreased level of oxygen typical for this age. The presence of *Cerbia tabulata* and *Aptea eisenacki* and increase in *A. polymorpha* confirm the dating for the interval (Costa & Davey, 1992). The presence of *Vesperopsis mayi* is typical for the northern latitudes (Nøhr-Hansen, 1993) and tentatively suggest stressed environment (Harding & Allen, 1995).

The Early Aptian is confirmed with the presence of the red stained foraminifera and LAD of *Ctenidodinium elegantulum*, *Sirmiodinium grossii*, and *Pseudoceratium pelliferum* (Costa & Davey, 1992). The pronounce spike increase in gamma (Figure A1), together with abundant influx of bisaccate pollen grains and sapropelic organic in core, confirms the presence of OAE1 sediments, representing Selli event (Ainsworth et al., 2000). This interval is an equivalent to Fischschiefer bed in North Sea. The presence of *Subtilisphaera perlucida* is additional evidence of anoxic environment and confirms the age interpretation.

The presence of Barremian sediments within the section is supported with the downward change of the log pattern (Figure A1) and is confirmed with the LAD of *Aptea anaphrissa* and *Nelchinopsis kostromiensis*, together with the base of abundant presence of *P. cretaceum* and overall assemblage change (Costa & Davey, 1992).

A2. Coniacian-Albian Interval

The Lysing Formation, typically representing Turonian-Late Coniacian strata, is not prominently expressed in the log profile and has not been analyzed for biostratigraphy (Figure A1). The underlying interval is characterized by the rich assemblage indicative of Turonian age, present in two samples (Figure A1). The cooccurrence of acme event of *Palaeohystriophora infusorioides* together with abundance of

Cauverdinium membraniphorum is indicative of latest Turonian (Costa & Davey, 1992; Olde et al., 2014). The cooccurring *Stephodinium coronatum* and *Aptedinium maculatum* serve as important markers as their LAD are observed at top Turonian boundary (Costa & Davey, 1992), specifically for North Træna and Møre Basins (Radmacher et al., 2015; Smelror et al., 1994). The cooccurring *Heterosphaeridium difficile* is known to have its FAD within the Turonian (Costa & Davey, 1992), specifically in the North Træna Basin (Radmacher et al., 2015). The influx of *Surculosphaeridium longifurcatum*, observed in the sample below, is known to be characteristic of mid-Turonian strata (Costa & Davey, 1992; Radmacher et al., 2015).

Due to its lower thickness in comparison to the known sections of the basin, the Turonian interval of the well is considered to be either condensed or possessing a stratigraphic unconformity. Since the studied assemblages possess strong Middle-Late Turonian marker events and lack any Early Turonian events, this negative evidence is tentatively suggesting the presence of unconformity with the Early and partly Middle Turonian intervals missing from the section.

The underlying part of the Blålange Formation is characterized by extensively expanded section with its age defined in two samples from the upper part of the studied interval (Figure A1). The assemblage in these samples is represented by the abundant presence of *Subtilisphaera kalaatii* and other peridinoid cysts such as *Palaeoperidinium cretaceum* and *Palaeohystrichophora infusoroides*, together with increase of common *Chlamydophorella nyei* and single occurrences of *Rhombodella paucispina* and *Ovoidinium scabrosum*. These events suggest the correlation to the Palaeohystrichophora infusoroides-Paaehystrichophora palaeoinfusa Interval Zone in the sense of Radmacher et al. (2014) and are indicative of Middle-Late Cenomanian.

The presence of the assemblages dominated with peridinoid cysts, specifically *Palaeoperidinium cretaceum* and *Subtilisphaera kalaatii*, in Cenomanian strata is characteristic for North Træna Basin (Radmacher et al., 2015), southwestern Barents Sea (Radmacher et al., 2014), and East Greenland (Nøhr-Hansen, 1993, 2012).

Appendix B: A Comment on the Petrophysical Properties Used in the 2-D Potential Field Modeling of the Northern Vørings Transect

All potential field studies combine a priori constraints such as physical property data, geological mapping, or seismic interpretations to limit the infinite number of possible theoretical solutions (Saltus & Blakely, 2011). Some of the modeling assumptions derived mostly (1) from local onshore-offshore correlations of some gravity and magnetic anomalies, (2) the nature of the rocks expected, (3) the correlation with V_p values from refraction/OBS data, and (4) the conclusion of the potential field modeling itself.

Rock property data from onshore (see NGU database) (e.g., Olesen et al., 2010) and local offshore density logs also provide local constrains, but mostly limited to the upper part of the sedimentary basin and/or the proximal part of the margin. We assume that the density in the deepest part of the basin does not exceed an average value of $2,750 \text{ kg/m}^3$, which also fits conventional V_p /density function. This threshold value was also voluntarily chosen to reach the maximum of crustal thinning we could expect along the transect.

Sedimentary rocks are also almost nonmagnetic (e.g., Olesen et al., 2010), and we assumed, accordingly, that most of the magnetic sources source from the crystalline basement or the basalt in the outer part of the margin.

Review of the onshore measurements (see Olesen et al., 2010) shows a large variation of the rock properties. However, all rocks from the upper part of the crust (e.g., the Caledonian nappes) have, in average, lower density and lower magnetic susceptibilities ($<0.01\text{--}0.02 \text{ SI}$) compared to the pre-Cambrian crust showing higher density and much higher susceptibilities ($>0.03 \text{ SI}$). Previous modelings have shown that a simple crustal model with an upper crust dominated by rocks equivalent of the Caledonian nappes and a magnetic middle crust associated with pre-Cambrian types of rocks could easily explain the observed gravity and magnetic signature of the mid-Norwegian Margin (e.g., Ebbing et al., 2006; Gernigon et al., 2015; Maystrenko et al., 2017; Olesen et al., 2010; Reynisson et al., 2010). The lower to the upper crust with V_p velocities higher than 7 km/s are most likely characterized by high-density material as confirmed by our modeling (e.g., the prominent gravity anomaly of the Utgard High). In general, the crustal densities are also realistic and remain in the range of average crustal values measured at specific depth on the Earth (Christensen & Mooney, 1995; Herzberg et al., 1983).

In addition to the forward modeling, we also consider Werner independent deconvolution techniques to estimate the potential field sources directly from measured anomalies without appeal to specific assumptions about the source distributions. When finally combined with seismic data, the final potential field model fits all observations and geophysical data available (e.g., seismic, gravity, and magnetic). Therefore, if a model produces results that agree with data, we will regard it as successful until new data and understanding allow us to modify or even reject modeling results. The parameters in Table 1 just show the best parameters required to fit all the data and observations. Without extra constrain, a sensitivity analysis will only result in a minor variation of the relative crustal properties involved.

Acknowledgments

Funding for this work came from OMNIS Project: Offshore Mid-Norwegian: Integrated Margin and Basin Studies (project: 210429/E30) funded by the Norwegian Research Council through its Centre of Excellence CEED (Centre for Earth Evolution and Dynamics). The seismic, magnetic, and gravity data presented in this study were provided by TGS. RPS Ichron is acknowledged for performing biostratigraphic analysis of well 6608/2-1S. Seismic interpretation was done using IHS Kingdom software. Grid interpolations and map compilations were established using Geosoft Oasis Montaj and ArcGIS softwares. We would like to acknowledge First Geo AS and TGS for the use of hiQbe™ regional velocity cube employed in depth conversion. We thank GeoModelling Solutions for providing an academic license for TecMod 2-D software. The seismic and well data used in this study are available through the Diskos National Data Repository (NDR). Well formation tops are also available at the NPD factpages (www.npd.no) and the NORLEX team website (www.nhm2.uit.no/norlex/). We are grateful to Jolante van Wijk (New Mexico Tech), Daniel Schmid (PGP, University of Oslo), and Sergei Medvedev (CEED, University of Oslo) for their help and fruitful discussions that improved the paper, and we thank Ben Manton (VBPR) for the linguistic remarks. We also would like to thank Christopher Jackson, Philip Ball, and the Editor Nathan Niemi for their constructive and helpful reviews.

References

- Abdelmalak, M. M., Andersen, T. B., Planke, S., Faleide, J. I., Corfu, F., Tegner, C., ... Myklebust, R. (2015). The ocean-continent transition in the mid-Norwegian margin: Insight from seismic data and an onshore Caledonian field analogue. *Geology*, 43(11), 1011–1014. <https://doi.org/10.1130/G37086.1>
- Abdelmalak, M. M., Faleide, J. I., Planke, S., Gernigon, L., Zastrozhnov, D., Shephard, G. E., & Myklebust, R. (2017). The T-Reflection and the deep crustal structure of the Vøring Margin offshore mid-Norway. *Tectonics*, 36, 2497–2523. <https://doi.org/10.1002/2017TC004617>
- Abdelmalak, M. M., Meyer, R., Planke, S., Faleide, J. I., Gernigon, L., Frieling, J., ... Myklebust, R. (2016). Pre-breakup magmatism on the Vøring Margin: Insight from new sub-basalt imaging and results from Ocean Drilling Program Hole 642E. *Tectonophysics*, 675, 258–274. <https://doi.org/10.1016/j.tecto.2016.02.037>
- Abdelmalak, M. M., Planke, S., Faleide, J. I., Jerram, D. A., Zastrozhnov, D., Eide, S., & Myklebust, R. (2016). The development of volcanic sequences at rifted margins: New insights from the structure and morphology of the Vøring Escarpment, mid-Norwegian Margin. *Journal of Geophysical Research: Solid Earth*, 121, 5212–5236. <https://doi.org/10.1002/2015JB012788>
- Ainsworth, N. R., Riley, L. A., & Gallagher, L. T. (2000). An Early Cretaceous lithostratigraphic and biostratigraphic framework for the Britannia Field reservoir (Late Barremian–Late Aptian), UK North Sea. *Petroleum Geoscience*, 6(4), 345–367. <https://doi.org/10.1144/petgeo.6.4.345>
- Allen, P. A., & Allen, J. R. (2013). *Basin analysis: Principles and application to petroleum play assessment* (p. 642). Chichester: John Wiley.
- Anderson, J. A. (1986). Arctic geodynamics: The opening of the Arctic Ocean. *Advances in Space Research*, 6(9), 79–83. [https://doi.org/10.1016/0273-1177\(86\)90356-X](https://doi.org/10.1016/0273-1177(86)90356-X)
- Bergh, S. G., Eig, K., Kløvjan, O. S., Henningsen, T., Olesen, O., & Hansen, J. A. (2007). The Lofoten-Vesterålen continental margin: A multiphase Mesozoic-Palaeogene rifted shelf as shown by offshore-onshore brittle fault-fracture analysis. *Norwegian Journal of Geology*, 87, 29–58.
- Berndt, C., Skogly, O. P., Planke, S., Eldholm, O., & Mjelde, R. (2000). High-velocity breakup-related sills in the Vøring Basin, off Norway. *Journal of Geophysical Research*, 105, 28, 443–28, 454. <https://doi.org/10.1029/2000JB900217>
- Bjørnseth, H. M., Grant, S. M., Hansen, E. K., Hossack, J. R., Roberts, D. G., & Thompson, M. (1997). Structural evolution of the Vøring Basin, Norway, during the Late Cretaceous and Paleogene. *Journal of the Geological Society (London)*, 154(3), 559–563. <https://doi.org/10.1144/gsjgs.154.3.0559>
- Blystad, P., Brekke, H., Færseth, R. B., Larsen, B. T., Skogseid, J., & Tørudbakken, B. (1995). Structural elements of the Norwegian continental shelf. Part II: The Norwegian Sea region. *NPD-Bulletin*, The Norwegian Petroleum Directorate, 8.
- Brekke, H. (2000). The tectonic evolution of the Norwegian Sea continental margin with emphasis on the Voring and Møre Basins. *Geological Society, London, Special Publications*, 167(1), 327–378. <https://doi.org/10.1144/gsl.sp.2000.167.01.13>
- Brekke, H., Dahlgren, S., Nyland, B., & Magnus, C. (1999). The prospectivity of the Vøring and Møre Basins on the Norwegian Sea continental margin. *Geological Society, London, Petroleum Geology Conference series*, 5, 261–274. <https://doi.org/10.1144/0050261>
- Brekke, H., & Riis, F. (1987). Tectonics and basin evolution of the Norwegian shelf between 62°N and 72°N. *Norsk Geologisk Tidsskrift*, 67, 295–322.
- Brune, S., Heine, C., Perez-Gussinyé, M., & Sobolev, S. V. (2014). Rift migration explains continental margin asymmetry and crustal hyper-extension. *Nature Communications*, 5. <https://doi.org/10.1038/ncomms5014>
- Brune, S., Popov, A. A., & Sobolev, S. V. (2012). Modeling suggests that oblique extension facilitates rifting and continental break-up. *Journal of Geophysical Research*, 117, B08402. <https://doi.org/10.1029/2011JB008860>
- Brune, S., Williams, S. E., Butterworth, N. P., & Müller, R. D. (2016). Abrupt plate accelerations shape rifted continental margins. *Nature*, 536(7615), 201–204. <https://doi.org/10.1038/nature18319>
- Buck, W. R. (2006). The role of magma in the development of the Afro-Arabian rift system. In G. Yirgu, C. J. Ebinger, & P. K. H. Maguire (Eds.), *The Afar Volcanic Province within the East African Rift System*, Geological Society, London, Special Publications (Vol. 259, pp. 43–54). <https://doi.org/10.1144/GSL.SP.2006.259.01.05>
- Chian, D., Reid, I. D., & Jackson, H. R. (2001). Crustal structure beneath Orphan Basin and implications for nonvolcanic continental rifting. *Journal of Geophysical Research*, 106(B6), 10,923–10,940. <https://doi.org/10.1029/2000JB900422>
- Christensen, N. I., & Mooney, W. D. (1995). Seismic velocity structure and composition of the continental crust: A global view. *Journal of Geophysical Research*, 100(B6), 9761–9788. <https://doi.org/10.1029/95JB00259>
- Christie-Blick, N., & Biddle, K. T. (1985). Deformation and basin formation along strike-slip faults. *SEPM Special Publication*, 37, 1–34. <https://doi.org/10.2110/pec.85.37.0001>
- Clark, S. A., Glørstad-Clark, E., Faleide, J. I., Schmid, D., Hartz, E. H., & Fjeldskaar, W. (2014). Southwest Barents Sea rift basin evolution: Comparing results from backstripping and time-forward modelling. *Basin Research*, 26(4), 550–566. <https://doi.org/10.1111/bre.12039>
- Clerc, C., Lagabrielle, Y., Labaume, P., Ringenbach, J.-C., Vauchez, A., Nalpas, T., ... Fourcade, S. (2016). Basement-cover decoupling and progressive exhumation of metamorphic sediments at hot rifted margin. Insights from the Northeastern Pyrenean analog. *Tectonophysics*, 686, 82–97. <https://doi.org/10.1016/j.tecto.2016.07.022>
- Clerc, C., Lahfid, A., Monié, P., Lagabrielle, Y., Chopin, C., Poujol, M., ... de St Blanquat, M. (2015). High-temperature metamorphism during extreme thinning of the continental crust: Areappraisal of the north Pyrenean paleo-passive margin. *Solid Earth*, 6(2), 643–668. <https://doi.org/10.5194/se-6-643-2015>
- Clerc, C., Ringenbach, J.-C., Jolivet, L., & Ballard, J.-F. (2017). Rifted margins: Ductile deformation, boudinage, continentward-dipping normal faults and the role of the weak lower crust. *Gondwana Research*. <https://doi.org/10.1016/j.gr.2017.04.030>
- Cohen, K. M., Finney, S. C., Gibbard, P. L., & Fan, J.-X. (2013). The ICS international chronostratigraphic chart. *Episodes*, 36(3), 199–204.

- Corfield, S., Murphy, N., & Parker, S. (1999). The structural and stratigraphic framework of the Irish Rockall Trough. *Geological Society, London, Petroleum Geology Conference Series*, 5, 407–420. <https://doi.org/10.1144/0050407>
- Costa, L. I., & Davey, R. J. (1992). Dinoflagellate cysts of the Cretaceous system. In A. J. Powell (Ed.), *A stratigraphic index of dinoflagellate cysts* (pp. 99–131). London: Chapman & Hall. https://doi.org/10.1007/978-94-011-2386-0_3
- Dalland, A., Worsley, D., & Ofstad, K. (1988). A lithostratigraphic scheme for the Mesozoic and Cenozoic succession offshore mid- and northern Norway. *NPD Bulletin*, 4, 63.
- Dean, K., McLachlan, K., & Chambers, A. (1999). Rifting and the development of the Faeroe–Shetland Basin. *Geological Society, London, Petroleum Geology Conference Series*, 5, 533–544. <https://doi.org/10.1144/0050533>
- Digranes, P., Mjelde, R., Kodaira, S., Shimamura, H., Kanazawa, T., Shiobara, H., & Berg, E. W. (1998). A regional shear-wave velocity model in the central Vøring Basin, N. Norway, using three-component ocean bottom seismographs. *Tectonophysics*, 293(3–4), 157–174. [https://doi.org/10.1016/S0040-1951\(98\)00093-6](https://doi.org/10.1016/S0040-1951(98)00093-6)
- Doré, A. G., Lundin, E. R., Jensen, L. N., Birkland, Ø., Eliassen, P. E., & Fichler, C. (1999). Principal tectonic events in the evolution of the northwest European Atlantic margin. *Geological Society, London, Petroleum Geology Conference Series*, 5, 41–61. <https://doi.org/10.1144/0050041>
- Doré, A. G., Lundin, E. R., Kusznir, N. J., & Pascal, C. (2008). Potential mechanisms for the genesis of Cenozoic domal structures on the NE Atlantic margin: Pros and cons and some new ideas. In H. Johnson, et al. (Eds.), *The nature and origin of compression in passive margins*. Geological Society, London, Special Publications (Vol. 306, pp. 1–26). <https://doi.org/10.1144/SP306.1>
- Ebbing, J., Lundin, E., Olesen, O., & Hansen, E. K. (2006). The mid-Norwegian margin: A discussion of crustal lineaments, mafic intrusions, and remnants of the Caledonian root by 3D density modelling and structural interpretation. *Journal of the Geological Society, London*, 163(1), 47–59. <https://doi.org/10.1144/0016-764905-029>
- Ebinger, C., & Casey, M. (2001). Continental breakup in magmatic provinces: An Ethiopian example. *Geology*, 29(6), 527–530. [https://doi.org/10.1130/0091-7613\(2001\)029<0527:CBIMPA>2.0.CO;2](https://doi.org/10.1130/0091-7613(2001)029<0527:CBIMPA>2.0.CO;2)
- Eldholm, O., Thiede, J., & Taylor, E. (1989). Evolution of the Vøring volcanic margin. In O. Eldholm, J. Thiede, & E. Taylor (Eds.), *Proceedings of the Ocean Drilling Program, scientific results* (pp. 1033–1065). College Station, TX: Ocean Drilling Program.
- Eldholm, O., Tsikalas, F., & Faleide, J. I. (2002). Continental margin off Norway 62–75°N: Palaeogene tectono-magmatic segmentation and sedimentation. *Geological Society of London, Special Publication*, 197(1), 39–68. <https://doi.org/10.1144/gsl.sp.2002.197.01.03>
- Færseth, R. B. (2012). Structural development of the continental shelf offshore Lofoten–Vesterålen, northern Norway. *Norwegian Journal of Geology*, 92, 19–40.
- Færseth, R. B., & Lien, T. (2002). Cretaceous evolution in the Norwegian Sea—A period characterized by tectonic quiescence. *Marine and Petroleum Geology*, 19(8), 1005–1027. [https://doi.org/10.1016/S0264-8172\(02\)00112-5](https://doi.org/10.1016/S0264-8172(02)00112-5)
- Faleide, J. I., Tsikalas, F., Breivik, A. J., Mjelde, R., Ritzmann, O., Engen, Ø., ... Eldholm, O. (2008). Structure and evolution of the continental margin off Norway and the Barents Sea. *Episodes*, 31(1), 82–91.
- Faleide, J. I., Vågnes, E., & Gudlaugsson, S. T. (1993). Late Mesozoic-Cenozoic evolution of the southwestern Barents Sea in a regional rift-shear tectonic setting. *Marine and Petroleum Geology*, 10(3), 186–214. [https://doi.org/10.1016/0264-8172\(93\)90104-Z](https://doi.org/10.1016/0264-8172(93)90104-Z)
- Fjellanger, E., Surlyk, F., Wamsteeker, L. C., & Midtun, T. (2005). Upper Cretaceous basin-floor fans in the Vøring Basin, mid-Norway shelf. In B. Wandås, et al. (Eds.), *Onshore-offshore relationships on the North Atlantic Margin*, Norwegian Petroleum Society Special Publications (Vol. 12, pp. 135–164). [https://doi.org/10.1016/S0928-8937\(05\)80047-5](https://doi.org/10.1016/S0928-8937(05)80047-5)
- Foulger, G. R. (2010). *Plates vs plumes: A geological controversy*. Oxford: Wiley-Blackwell. <https://doi.org/10.1002/9781444324860>
- Franke, D. (2013). Rifting, lithosphere breakup and volcanism: Comparison of magma-poor and volcanic rifted margins. *Marine and Petroleum Geology*, 43, 63–87. <https://doi.org/10.1016/j.marpetgeo.2012.11.003>
- Franke, D., Savva, D., Pubellier, M., Steuer, S., Mouly, B., Auzietre, J. L., ... Chamot-Rooke, N. (2014). The final rifting evolution in the South China Sea. *Marine and Petroleum Geology*, 58, 704–720. <https://doi.org/10.1016/j.marpetgeo.2013.11.020>
- Funck, T., Andersen, M. S., Neish, J. K., & Dahl-Jensen, T. (2008). A refraction seismic transect from the Faroe Islands to the Hatton-Rockall Basin. *Journal of Geophysical Research*, 113, B12405. <https://doi.org/10.1029/2008JB005675>
- Gartrell, A. P. (1997). Evolution of rift basins and low-angle detachments in multilayer analog models. *Geology*, 25(7), 615–618. [https://doi.org/10.1130/0091-7613\(1997\)025<0615:EORBAL>2.3.CO;2](https://doi.org/10.1130/0091-7613(1997)025<0615:EORBAL>2.3.CO;2)
- Geoffroy, L., Burov, E. B., & Werner, P. (2015). Volcanic passive margins: Another way to break up continents. *Scientific Reports*, 5. <https://doi.org/10.1038/srep14828>
- Gernigon, L., Blischke, A., Nasuti, A., & Sand, M. (2015). Conjugate volcanic rifted margins, seafloor spreading, and microcontinent: Insights from new high-resolution aeromagnetic surveys in the Norway Basin. *Tectonics*, 34, 907–933. <https://doi.org/10.1002/2014TC003717>
- Gernigon, L., Brönnér, M., Roberts, D., Olesen, O., Nasuti, A., & Yamasaki, T. (2014). Crustal and basin evolution of the southwestern Barents Sea: From Caledonian orogeny to continental breakup. *Tectonics*, 33, 347–373. <https://doi.org/10.1002/2013TC003439>
- Gernigon, L., Ringenbach, J.-C., Planke, S., & Jonquet-Kolsto, H. (2003). Extension, crustal structure and magmatism at the outer Vøring Basin, Norwegian Margin. *Journal of Geological Society*, 160(2), 197–208. <https://doi.org/10.1144/0016-764902-055>
- Gernigon, L., Ringenbach, J.-C., Planke, S., & Le Gall, B. (2004). Deep structures and breakup along volcanic rifted margins: Insights from integrated studies along the outer Vøring Basin (Norway). *Marine and Petroleum Geology*, 21(3), 363–372. <https://doi.org/10.1016/j.marpetgeo.2004.01.005>
- Gomez, M., Verges, J., Fernandez, M., Torne, M., Ayala, C., Wheeler, W., & Karpuz, R. (2004). Extensional geometry of the Mid-Norwegian Margin before Early Tertiary continental breakup. *Marine and Petroleum Geology*, 21(2), 177–194. <https://doi.org/10.1016/j.marpetgeo.2003.11.017>
- Gradstein, F. M., Anthonissen, E., Brunstad, H., Charnock, M., Hammer, Ø., Hellem, T., & Lervik, K. S. (2010). Norwegian Offshore Stratigraphic Lexicon (NORLEX). *Newsletters on Stratigraphy*, 44(1), 73–86. <https://doi.org/10.1127/0078-0421/2010/0005>
- Grant, N., Bouma, A., & McIntyre, A. (1999). The Turonian play in the Faeroe–Shetland Basin. *Geological Society, London, Petroleum Geology Conference Series*, 5, 661–673. <https://doi.org/10.1144/0050661>
- Harding, I., & Allen, R. (1995). Dinocysts and the palaeoenvironmental interpretation of non-marine sediments: An example from the Wealden of the Isle of Wight (Lower Cretaceous, southern England). *Cretaceous Research*, 16(6), 727–743. <https://doi.org/10.1006/cres.1995.1046>
- Harry, D. L., & Bowling, J. C. (1999). Inhibiting magmatism on nonvolcanic rifted margins. *Geology*, 27(10), 895–898. [https://doi.org/10.1130/0091-7613\(1999\)027<0895:IMONRM>2.3.CO;2](https://doi.org/10.1130/0091-7613(1999)027<0895:IMONRM>2.3.CO;2)
- Henstra, G. A., Gawthorpe, R. L., Helland-Hansen, W., Ravnås, R., & Rottevatn, A. (2016). Depositional systems in multiphase rifts: Seismic case study from the Lofoten margin, Norway. *Basin Research*, 29(4), 447–469. <https://doi.org/10.1111/bre.12183>
- Herzberg, C. T., Fyfe, W. S., & Carr, M. J. (1983). Density constraints on the formation of the continental Moho and crust. *Contributions to Mineralogy and Petrology*, 84(1), 1–5. <https://doi.org/10.1007/BF01132324>

- Hjelstuen, B. O., Eldholm, O., & Skogseid, J. (1999). Cenozoic evolution of the northern Vøring Margin. *Geological Society of America Bulletin*, 111(12), 1,792–1,807. [https://doi.org/10.1130/0016-7606\(1999\)111<1792:CEOTNV>2.3.CO;2](https://doi.org/10.1130/0016-7606(1999)111<1792:CEOTNV>2.3.CO;2)
- Huismans, R. S., & Beaumont, C. (2011). Depth-dependent extension, two-stage breakup and cratonic underplating at rifted margins. *Nature*, 473(7,345), 74–78. <https://doi.org/10.1038/nature09988>
- Imber, J., Holdsworth, R. E., McCaffrey, K. J. W., Wilson, R. W., Jones, R. R., England, R. W., & Gjeldvik, G. (2005). Early Tertiary sinistral transpression and fault reactivation in the western Vøring Basin, Norwegian Sea: Implications for hydrocarbon exploration and pre-breakup deformation in ocean margin basins. *AAPG Bulletin*, 89(8), 1043–1069. <https://doi.org/10.1306/02240504043>
- Kjennerud, T., & Vergara, L. (2005). Cretaceous to Palaeogene 3D palaeobathymetry and sedimentation in the Vøring Basin, Norwegian Sea. In A. G. Doré & B. A. Vining (Eds.), *Petroleum geology: Northwest Europe and global perspectives—Proceedings of the 6th Petroleum Geology Conference* (pp. 815–831). Geological Society, London.
- Kusznir, N. J., Hunsdale, R., Roberts, A. M., & iSIMM Team (2005). Timing and magnitude of depth-dependent lithosphere stretching on the S. Lofoten and N. Vøring continental margins offshore mid-Norway: Implications for subsidence and hydrocarbon maturation at volcanic rifted margins. In A. G. Doré & B. A. Vining (Eds.), *Petroleum geology: Northwest Europe and global perspectives, Proceedings of the 6th Petroleum Geology Conference* (pp. 767–783). Geological Society, London.
- Lavier, L. L., & Manatschal, G. (2006). A mechanism to thin the continental lithosphere at magma-poor margins. *Nature*, 440(7,082), 324–328. <https://doi.org/10.1038/nature04608>
- Lister, G. S., Etheridge, M. A., & Symonds, P. A. (1986). Detachment faulting and the evolution of passive continental margins. *Geology*, 14(3), 246–250. [https://doi.org/10.1130/0091-7613\(1986\)14<246:DFATEO>2.0.CO;2](https://doi.org/10.1130/0091-7613(1986)14<246:DFATEO>2.0.CO;2)
- Lundin, E. R., & Doré, A. G. (1997). A tectonic model for the Norwegian passive margin with implications for the NE Atlantic: Early Cretaceous to break-up. *Geological Society London Journal*, 154(3), 545–550. <https://doi.org/10.1144/gsjgs.154.3.0545>
- Lundin, E. R., & Doré, A. G. (2011). Hyperextension, serpentization, and weakening: A new paradigm for rifted margin compressional deformation. *Geology*, 39(4), 347–350. <https://doi.org/10.1130/G31499.1>
- Lundin, E. R., Doré, A. G., Ronning, K., & Kyrkjebo, R. (2013). Repeated inversion and collapse in the Late Cretaceous-Cenozoic northern Vøring Basin, offshore Norway. *Petroleum Geoscience*, 19(4), 329–341. <https://doi.org/10.1144/petgeo2012-022>
- Lundin, E. R., Ronning, K., Doré, A. G., & Olesen, O. (2002). Hel Graben, Vøring Basin, Norway—A possible major cauldron? Paper presented at 25th Nordic Geological Winter Meeting, 6–9 January, Reykjavik, Abstract Volume, 132.
- Maystrenko, Y. P., Olesen, O., Gernigon, L., & Gradmann, S. (2017). Deep structure of the Lofoten-Vesterålen segment of the mid-Norwegian continental margin and adjacent areas derived from 3-D density modeling. *Journal of Geophysical Research: Solid Earth*, 122, 1402–1433. <https://doi.org/10.1002/2016JB013443>
- McKenzie, D. (1978). Some remarks on the development of sedimentary basins. *Earth and Planetary Science Letters*, 40(1), 25–32. [https://doi.org/10.1016/0012-821X\(78\)90071-7](https://doi.org/10.1016/0012-821X(78)90071-7)
- Meyer, R., van Wijk, J., & Gernigon, L. (2007). The North Atlantic Igneous Province: A review of models for its formation. In G. R. Foulger & D. M. Jurdy (Eds.), *Plates, plumes and planetary processes*, Geological Society of America Special Paper (Vol. 430, pp. 525–552). [https://doi.org/10.1130/2007.2430\(26\)](https://doi.org/10.1130/2007.2430(26))
- Mjelde, R., Digranes, P., Shimamura, H., Shiobara, H., Kodaira, S., Brekke, S. H., ... Thorbjørnsen, T. (1998). Crustal structure of the northern part of the Vøring Basin, mid-Norway margin, from wide-angle seismic and gravity data. *Tectonophysics*, 293(3-4), 175–205. [https://doi.org/10.1016/S0040-1951\(98\)00090-0](https://doi.org/10.1016/S0040-1951(98)00090-0)
- Mjelde, R., Goncharov, A., & Müller, R. D. (2013). The Moho: Boundary above upper mantle peridotites or lower crustal eclogites? A global review and new interpretations for passive margins. *Tectonophysics*, 609, 636–650. <https://doi.org/10.1016/j.tecto.2012.03.001>
- Mjelde, R., Kodaira, S., Shimamura, H., Kanazawa, T., Shiobara, H., Berg, E. W., & Riise, O. (1997). Crustal structure of the central part of the Vøring Basin, mid-Norway margin, from ocean bottom seismographs. *Tectonophysics*, 277, 235–257. [https://doi.org/10.1016/S0040-1951\(97\)00028-0](https://doi.org/10.1016/S0040-1951(97)00028-0)
- Mjelde, R., Kvarven, T., Faleide, J. I., & Thybo, H. (2016). Lower crustal high-velocity bodies along North Atlantic passive margins, and their link to Caledonian suture zone eclogites and Early Cenozoic magmatism. *Tectonophysics*, 670, 16–29. <https://doi.org/10.1016/j.tecto.2015.11.021>
- Mjelde, R., Raum, T., Digranes, P., Shimamura, H., Shiobara, H., & Kodaira, S. (2003). V_p/V_s ratio along the Vøring Margin, NE Atlantic, derived from OBS data: Implications on lithology and stress field. *Tectonophysics*, 369(3-4), 175–197. [https://doi.org/10.1016/S0040-1951\(03\)00198-7](https://doi.org/10.1016/S0040-1951(03)00198-7)
- Mogensen, T. E., Nyby, R., Karpuz, R., & Haremo, P. (2000). Late Cretaceous and Tertiary structural evolution of the northeastern part of the Vøring Basin, Norwegian Sea. In A. Nøttvedt et al. (Eds.), *Dynamics of the Norwegian margin: Geological Society, London, Special Publication* (Vol. 167, pp. 379–396). <https://doi.org/10.1144/GSL.SP.2000.167.01.14>
- Morton, A. C., & Grant, S. (1998). Cretaceous depositional systems in the Norwegian Sea: Heavy mineral constraints. *AAPG Bulletin*, 82(2), 274–290.
- Mosar, J. (2000). Depth of extensional faulting on the Mid-Norway Atlantic passive margin. *Norgesgeologiske undersekelse Bulletin*, 437, 33–41.
- Mosar, J., Eide, E. A., Osmundsen, P. T., Sommeruga, A., & Torsvik, T. (2002). Greenland-Norway separation: A geodynamic model for the North Atlantic. *Norwegian Journal of Geology*, 82, 281–298.
- Neumann, E.-R., Svensen, H., Tegner, C., Plank, S., Thirlwall, M., & Jarvis, K. E. (2013). Sill and lava geochemistry of the mid-Norway and NE Greenland conjugate margins. *Geochemistry, Geophysics, Geosystems*, 14, 3666–3690. <https://doi.org/10.1002/ggge.20224>
- Ní Dheasúna, M., M. Ballesteros, J. Leven (2012). A regional velocity cube for depth conversion on the Northwest Shelf, PESA News Resources, August/September, 2012, 40–43. Retrieved from www.pnronline.com.au/article.aspx?p=1&id=810
- Nirrengarten, M., Gernigon, L., & Manatschal, G. (2014). Lower crustal bodies in the Møre volcanic rifted margin: Geophysical determination and geological implications. *Tectonophysics*, 636, 143–157. <https://doi.org/10.1016/j.tecto.2014.08.004>
- Nøhr-Hansen, H. (1993). Dinoflagellate cyst stratigraphy of the Barremian to Albian, Lower Cretaceous, North-East Greenland. *Bulletin. Grønlands Geologiske Undersøgelse*, 166, 1–171.
- Nøhr-Hansen, H. (2012). Palynostratigraphy of the Cretaceous–lower Palaeogene sedimentary succession in the Kangerlussuaq Basin, southern East Greenland. *Review of Palaeobotany and Palynology*, 178, 59–90. <https://doi.org/10.1016/j.revpalbo.2012.03.009>
- Norwegian Petroleum Directorate (NPD) (2017). Factpages. Retrieved from <http://factpages.npd.no/factpages/>, last access April 2017.
- Olde, K., Jarvis, I., Pearce, M. M., Uličný, D., Tocher, B., Trabucho-Alexandre, J., & Gröcke, D. (2014). A revised northern European Turonian (Upper Cretaceous) dinoflagellate cyst biostratigraphy: Integrating palynology and carbon isotope events. *Review of Palaeobotany and Palynology*, 213, 1–16.
- Olesen, O., Brönner, M., Ebbing, J., Gellein, J., Gernigon, L., Koziel, J., ... Usov, S. (2010). New aeromagnetic and gravity compilations from Norway and adjacent areas—Methods and applications. In B. A. Vining & S. C. Pickering (Eds.), *Petroleum geology: From mature basins*

- to new frontiers, proceedings of the 7th Petroleum Geology Conference (pp. 559–586). London: Geological Society. <https://doi.org/10.1144/0070559>
- Osmundsen, P. T., & Ebbing, J. (2008). Style of extension offshore mid-Norway and implications for mechanisms of crustal thinning at passive margins. *Tectonics*, 27, TC6016. <https://doi.org/10.1029/2007TC002242>
- Osmundsen, P. T., Péron-Pinvidic, G., Ebbing, J., Erratt, D., Fjellanger, E., Bergslien, D., & Syvertsen, S. E. (2016). Extension, hyperextension and mantle exhumation offshore Norway: A discussion based on 6 crustal transects. *Norwegian Journal of Geology*, 96, 343–372. <https://doi.org/10.1785/njg96-4-05>
- Osmundsen, P. T., Sommaruga, A., Skilbrei, J. R., & Olesen, O. (2002). Deep structure of the mid-Norway rifted margin. *Norwegian Journal of Geology*, 82, 205–224.
- Pascoe, R., Hooper, R., Storhaug, K., & Harper, H. (1999). Evolution of extensional styles at the southern termination of the Nordland Ridge, Mid-Norway: A response to variations in coupling above Triassic salt. *Geological Society, London, Petroleum Geology Conference Series*, 5, 83–90. <https://doi.org/10.1144/0050083>
- Pérez-Gussinyé, M., & Reston, T. J. (2001). Rheological evolution during extension at nonvolcanic rifted margins: Onset of serpentinization and development of detachments leading to continental breakup. *Journal of Geophysical Research*, 106, 3961–3975. <https://doi.org/10.1029/2000JB900325>
- Péron-Pinvidic, G., Manatschal, G., & Osmundsen, P. T. (2013). Structural comparison of archetypal Atlantic rifted margins: A review of observations and concepts. *Marine and Petroleum Geology*, 43, 21–47. <https://doi.org/10.1016/j.marpetgeo.2013.02.002>
- Péron-Pinvidic, G., & Osmundsen, P. T. (2016). Architecture of the distal and outer domains of the mid-Norwegian rifted margin: Insights from the Råg-Gjallar ridges system. *Marine and Petroleum Geology*, 77, 280–299. <https://doi.org/10.1016/j.marpetgeo.2016.06.014>
- Petersen, K. D., & Schiffer, C. (2016). Wilson cycle passive margins: Control of orogenic inheritance on continental breakup. *Gondwana Research*, 39, 131–144. <https://doi.org/10.1016/j.gr.2016.06.012>
- Pinel, V., & Jaupart, C. (2005). Caldera formation by magma withdrawal from a reservoir beneath a volcanic edifice. *Earth and Planetary Science Letters*, 230(3–4), 273–287. <https://doi.org/10.1016/j.epsl.2004.11.016>
- Planke, S., Skogseid, J., & Eldholm, O. (1991). Crustal structure off Norway, 62–70°N. *Tectonophysics*, 189(1–4), 91–107. [https://doi.org/10.1016/0040-1951\(91\)90489-F](https://doi.org/10.1016/0040-1951(91)90489-F)
- Radmacher, W., Mangerud, G., & Tyszka, J. (2015). Dinoflagellate cyst biostratigraphy of Upper Cretaceous strata from two wells in the Norwegian Sea. *Review of Palaeobotany and Palynology*, 216, 18–32. <https://doi.org/10.1016/j.revpalbo.2014.12.007>
- Radmacher, W., Tyszka, J., Mangerud, G., & Pearce, M. A. (2014). Dinoflagellate cyst biostratigraphy of the Late Albian to Early Maastrichtian in the southwestern Barents Sea. *Marine and Petroleum Geology*, 57, 109–121. <https://doi.org/10.1016/j.marpetgeo.2014.04.008>
- Redfield, T. F., Braathen, A., Gabrielsen, R. H., Osmundsen, P. T., Torsvik, T., & Andriessen, P. A. M. (2005). Late Mesozoic to Early Cenozoic components of vertical separation across the Møre Trøndelag Fault Complex, Norway. *Tectonophysics*, 395(3–4), 233–249. <https://doi.org/10.1016/j.tecto.2004.09.012>
- Ren, S., Faleide, J. I., Eldholm, O., Skogseid, J., & Gradstein, F. (2003). Late Cretaceous–Paleocene development of the NW Vøring Basin. *Marine and Petroleum Geology*, 20(2), 177–206. [https://doi.org/10.1016/S0264-8172\(03\)00005-9](https://doi.org/10.1016/S0264-8172(03)00005-9)
- Ren, S., Skogseid, J., & Eldholm, O. (1998). Late Cretaceous–Paleocene extension on the Vøring volcanic margin. *Marine Geophysical Researches*, 20(4), 343–369. <https://doi.org/10.1023/A:1004554217069>
- Reynisson, R. F., Ebbing, J., Lundin, E., & Osmundsen, P. T. (2010). Properties and distribution of lower crustal bodies on the mid-Norwegian margin. *Geological Society, London, Petroleum Geology Conference Series*, 7, 843–854. <https://doi.org/10.1144/0070843>
- Rise, L., Ottesen, D., Berg, K., & Lundin, E. (2005). Large-scale development of the mid-Norwegian margin during the last 3 million years. *Marine and Petroleum Geology*, 22(1–2), 33–44. <https://doi.org/10.1016/j.marpetgeo.2004.10.010>
- Roberts, A. M., Corfield, R. I., Kusznir, N. J., Matthews, S. J., Hansen, E.-K., & Hooper, R. J. (2009). Mapping palaeostructure and palaeobathymetry along the Norwegian Atlantic continental margin, Møre and Vøring basins. *Petroleum Geoscience*, 15(1), 27–43. <https://doi.org/10.1144/1354-079309-804>
- Rosenbaum, G., Regenauer-Lieb, K., & Weinberg, R. F. (2010). Interaction between mantle and crustal detachments: A nonlinear system controlling lithospheric extension. *Journal of Geophysical Research*, 115, B11412. <https://doi.org/10.1029/2009JB006696>
- Rüpke, L. H., Schmalholz, S. M., Schmid, D. W., & Podladchikov, Y. Y. (2008). Automated thermotectonostratigraphic basin reconstruction: Viking Graben case study. *AAPG Bulletin*, 92(3), 309–326. <https://doi.org/10.1306/11140707009>
- Rüpke, L. H., Schmid, D. W., Hartz, E. H., & Martinsen, B. (2010). Basin modelling of a transform margin setting: Structural, thermal and hydrocarbon evolution of the Tano Basin, Ghana. *Petroleum Geoscience*, 16(3), 283–298. <https://doi.org/10.1144/1354-079309-905>
- Rüpke, L. H., Schmid, D. W., Perez-Gussinyé, M., & Hartz, E. (2013). Interrelation between rifting, faulting, sedimentation, and mantle serpentinization during continental margin formation—including examples from the Norwegian Sea. *Geochemistry, Geophysics, Geosystems*, 14, 4351–4369. <https://doi.org/10.1002/ggge.20268>
- Saltus, R. W., & Blakely, R. J. (2011). Unique geologic insights from “non-unique” gravity and magnetic interpretation. *GSA Today*, 21(12), 4–10. <https://doi.org/10.1130/G136A.1>
- Scheck-Wenderoth, M., & Maystrenko, Y. P. (2011). 3D lithospheric-scale structural model of the Norwegian continental margin (the Vøring and Møre basins). *Scientific Technical Report STR11/02-Data*, GFZ Potsdam. <https://doi.org/10.2312/GFZ.b103-11027>
- Scheck-Wenderoth, M., Raum, T., Faleide, J. I., Mjelde, R., & Horsfield, B. (2007). The transition from the continent to the ocean: A deeper view on the Norwegian margin. *Journal of the Geological Society of London*, 164(4), 855–868. <https://doi.org/10.1144/0016-76492006-131>
- Serck, C. S., Faleide, J. I., Braathen, A., Kjølhamar, B., & Escalona, A. (2017). Jurassic to Early Cretaceous basin configuration (s) in the Fingerdjupet subbasin, SW Barents Sea. *Marine and Petroleum Geology*, 86, 874–891. <https://doi.org/10.1016/j.marpetgeo.2017.06.044>
- Simon, K., Huismans, R. S., & Beaumont, C. (2009). Dynamical modelling of lithospheric extension and small-scale convection: Implications for magmatism during the formation of volcanic rifted margins. *Geophysical Journal International*, 176(1), 327–350. <https://doi.org/10.1111/j.1365-246X.2008.03891.x>
- Skogseid, J., Eldholm, O., & Larsen, V. B. (1992). Vøring Basin: Subsidence and tectonic evolution. In R. M. Larsen, et al. (Eds.), *Structural and tectonic modeling and its application to petroleum geology, Norwegian Petroleum Society, Special Publications* (Vol. 1, pp. 55–82). Elsevier, Amsterdam.
- Skogseid, J., Planke, S., Faleide, J. I., Pedersen, T., Eldholm, O., & Neverdal, F. (2000). NE Atlantic continental rifting and volcanic margin formation. In A. Nøttvedt et al. (Eds.), *Dynamics of the Norwegian margin*, Geological Society, London, Special Publication (Vol. 167, pp. 295–326). Geological Society, London. <https://doi.org/10.1144/GSL.SP.2000.167.01.12>
- Slagstad, T., Davidsen, B., & Daly, J. S. (2011). Age and composition of crystalline basement rocks on the Norwegian continental margin: Offshore extension and continuity of the Caledonian–Appalachian orogenic belt. *Journal of the Geological Society, London*, 168(5), 1167–1185. <https://doi.org/10.1144/0016-76492010-136>

- Smelror, M., Jacobsen, T., Rise, L., Skarbø, O., Verdenius, J. G., & Vigran, J. O. (1994). Jurassic to Cretaceous stratigraphy of shallow cores on the Møre Basin Margin, Mid-Norway. *Norsk Geologisk Tidsskrift*, 74, 89–107.
- Sømme, T. O., & Jackson, C. A. L. (2013). Source-to-sink analysis of ancient sedimentary systems using a subsurface case study from the Møre–Trøndelag area of southern Norway: Part 2—Sediment dispersal and forcing mechanisms. *Basin Research*, 25, 512–531. <https://doi.org/10.1111/bre.12014>
- Sun, Z., Zhou, D., Wu, S. M., Zhong, Z. H., Myra, K., Jiang, J. Q., & Fan, H. (2009). Patterns and dynamics of rifting on passive continental margin from shelf to slope of the northern South China Sea: Evidence from 3D analogue modeling. *Journal of Earth Science China*, 20(1), 136–146. <https://doi.org/10.1007/s12583-009-0011-6>
- Swiecicki, T., Gibbs, P. B., Farrow, G. E., & Coward, M. P. (1998). A tectonostratigraphic framework for the mid-Norway region. *Marine and Petroleum Geology*, 15(3), 245–276. [https://doi.org/10.1016/S0264-8172\(97\)00029-9](https://doi.org/10.1016/S0264-8172(97)00029-9)
- Talwani, M. (1973). Computer usage in the computation of gravity anomalies. *Methods in Computational Physics*, 13, 343–389.
- Talwani, M., & Eldholm, O. (1977). Evolution of the Norwegian-Greenland Sea. *Bulletin Geological Society of America*, 88(7), 969–999. [https://doi.org/10.1130/0016-7606\(1977\)88<969:EOTNS>2.0.CO;2](https://doi.org/10.1130/0016-7606(1977)88<969:EOTNS>2.0.CO;2)
- ten Brink, U. S., & Ben-Avraham, Z. (1989). The anatomy of a pull-apart basin: Seismic reflection observations of the Dead Sea Basin. *Tectonics*, 8(2), 333–350. <https://doi.org/10.1029/TC0081002p00333>
- Theissen-Krah, S., & Rüpke, L. H. (2010). Feedbacks of sedimentation on crustal heat flow: New insights from the Vøring Basin, Norwegian Sea. *Basin Research*, 22, 976–990. <https://doi.org/10.1111/j.1365-2117.2009.00437>
- Theissen-Krah, S., Zastrozhnov, D., Abdelmalak, M. M., Schmid, D. W., Faleide, J. I., & Gernigon, L. (2017). Tectonic evolution and extension at the Møre Margin—Offshore mid-Norway. *Tectonophysics*, 721, 227–238. <https://doi.org/10.1016/j.tecto.2017.09.009>
- Thomsen, L. (1986). Weak elastic anisotropy. *Geophysics*, 51(10), 1954–1966. <https://doi.org/10.1190/1.1442051>
- Tsikalas, F., Faleide, J. I., & Eldholm, O. (2001). Lateral variations in tectono-magmatic style along the Lofoten-Vesterålen margin off Norway. *Marine and Petroleum Geology*, 18(7), 807–832. [https://doi.org/10.1016/S0264-8172\(01\)00030-7](https://doi.org/10.1016/S0264-8172(01)00030-7)
- Tsikalas, F., Faleide, J. I., Eldholm, O., & Wilson, J. (2005). Late Mesozoic–Cenozoic structural and stratigraphic correlations between the conjugate mid-Norway and NE Greenland continental margins. In A. G. Doré & B. A. Vining (Eds.), *Petroleum geology: Northwest Europe and global perspectives—Proceedings of the 6th Petroleum Geology Conference*, Geological Society, London (pp. 785–801). <https://doi.org/10.1144/0060785>
- Tsikalas, F., Faleide, J. I., & Kuznir, N. J. (2008). Along-strike variations in rifted margin crustal architecture and lithosphere thinning between northern Vøring and Lofoten margin segments off mid-Norway. *Tectonophysics*, 458(1–4), 68–81. <https://doi.org/10.1016/j.tecto.2008.03.001>
- Vågnes, E., Gabrielsen, R. H., & Haremo, P. (1998). Late Cretaceous-Cenozoic intraplate contractional deformation at the Norwegian continental shelf: Timing, magnitude and regional implications. *Tectonophysics*, 300(1–4), 29–46. [https://doi.org/10.1016/S0040-1951\(98\)00232-7](https://doi.org/10.1016/S0040-1951(98)00232-7)
- Van Avendonk, H. J. A., Lavier, L. L., Shillington, D. J., & Manatschal, G. (2009). Extension of continental crust at the margin of the eastern Grand Banks, Newfoundland. *Tectonophysics*, 468(1–4), 131–148. <https://doi.org/10.1016/j.tecto.2008.05.030>
- Van Wijk, J., Koning, D., Axen, G., Coblenz, D., Gragg, E., & Sion, B. (2018). Tectonic subsidence, geoid analysis, and the Miocene-Pliocene unconformity in the Rio Grande rift, southwestern United States: Implications for mantle upwelling as a driving force for rift opening. *Geosphere*. <https://doi.org/10.1130/GES01522.1>
- Van Wijk, J. W., Huismans, R. S., Ter Voorde, M., & Cloetingh, S. A. P. L. (2001). Melt generation at volcanic continental margins: No need for a mantle plume? *Geophysical Research Letters*, 28(20), 3995–3998. <https://doi.org/10.1029/2000GL012848>
- Vergara, L., Wreglesworth, I., Trayfoot, M., & Richardsen, G. (2001). The distribution of Cretaceous and Paleocene deep-water reservoirs in the Norwegian Sea basins. *Petroleum Geoscience*, 7(4), 395–408. <https://doi.org/10.1144/petgeo.7.4.395>
- Walker, I. M., Berry, K. A., Bruce, J. R., Bystøl, L., & Snow, J. H. (1997). Structural modelling of regional depth profiles in the Vøring Basin: Implications for the structural and stratigraphic development of the Norwegian passive margin. *Journal of the Geological Society, London*, 154(3), 537–544. <https://doi.org/10.1144/gsjgs.154.3.0537>
- Wangen, M., Mjelde, R., & Faleide, J. I. (2011). The extension of the Vøring margin (NE Atlantic) in case of different degrees of magmatic underplating. *Basin Research*, 23(1), 83–100. <https://doi.org/10.1111/j.1365-2117.2010.00467.x>
- White, N. J., & McKenzie, D. P. (1988). Formation of the “Steer’s Head” geometry of sedimentary basins by differential stretching of the crust and mantle. *Geology*, 16(3), 250–253. [https://doi.org/10.1130/0091-7613\(1988\)016<250:FOTSSH>2.3.CO;2](https://doi.org/10.1130/0091-7613(1988)016<250:FOTSSH>2.3.CO;2)
- White, R. S., Eccles, J. D., & Roberts, A. W. (2010). Constraints on volcanism, igneous intrusion and stretching on the Rockall–Faroe continental margin. *Petroleum Geology Conference Series*, 7, 831–842. <https://doi.org/10.1144/0070831>
- White, R. S., & McKenzie, D. P. (1989). Magmatism at rift zones: The generation of volcanic continental margins and flood basalts. *Journal of Geophysical Research*, 94(B6), 7685–7729. <https://doi.org/10.1029/JB094B06p07685>
- White, R. S., Smith, L. K., Roberts, A. W., Christie, P. A. F., Kusznir, N. J., & iSIMM Team (2008). Lower-crustal intrusion on the North Atlantic continental margin. *Nature*, 452(7186), 460–464. <https://doi.org/10.1038/nature06687>
- Whitham, A. G., Price, S. P., Koriani, A. M., & Kelly, S. R. A. (1999). Cretaceous (post-Valanginian) sedimentation and rift events in NE Greenland (71–77°N). *Geological Society, London, Petroleum Geology Conference Series*, 5, 325–336. <https://doi.org/10.1144/0050325>
- Xie, X., & Heller, P. L. (2009). Plate tectonics and basin subsidence history. *GSA Bulletin*, 121, 55–64. <https://doi.org/10.1130/B26398.1>
- Yamasaki, T., & Gernigon, L. (2009). Styles of lithospheric extension controlled by underplated mafic bodies. *Tectonophysics*, 468(1–4), 169–184. <https://doi.org/10.1016/j.tecto.2008.04.024>
- Yamasaki, T., & Gernigon, L. (2010). Redistribution of the lithosphere deformation by the emplacement of underplated mafic bodies: Implications for microcontinent formation. *Journal of the Geological Society of London*, 167(5), 961–971. <https://doi.org/10.1144/0016-76492010-027>